

**BIPED ROBOT REFERENCE GENERATION WITH NATURAL ZMP
TRAJECTORIES**

by
OKAN KURT

**Submitted to the Graduate School of Engineering and Natural Sciences
in partial fulfillment of the requirements for the degree of Master of Science**

Sabanci University

February 2006

**BIPED ROBOT REFERENCE GENERATION WITH NATURAL ZMP
TRAJECTORIES**

APPROVED BY:

Assist. Prof. Dr. Kemalettin Erbatur
(Thesis Advisor)

Prof. Dr. Asif Şabanoviç

Assoc. Prof. Dr. Mustafa Ünel

Assoc. Prof. Dr. Mahmut Akşit

Assist. Prof. Dr. Mujdat Cetin

DATE OF APPROVAL:

© Okan Kurt

2005

All Rights Reserved

ABSTRACT

Humanoid robotics attracted the attention of many researchers in the past 35 years. The motivation of research is the suitability of the biped structure for tasks in the human environment. The control of a humanoid robot is a challenging task due to the hard-to-stabilize dynamics.

Walking reference trajectory generation is a key problem. A criterion used for the reference generation is that the reference trajectory should be suitable to be followed by the robot with its natural dynamics with minimal control intervention. Reference generation techniques with the so-called Linear Inverted Pendulum Model (LIPM) are based on this idea. The Zero Moment Point (ZMP) Criterion is widely employed in the stability analysis of biped robot walk. Improved LIPM based reference generation methods obtained by applying the ZMP Criterion are reported too. In these methods, the ZMP during a stepping motion is kept fixed in the middle of the supporting foot sole, which lacks naturalness. In fact, the ZMP in the human walk does not stay fixed, but it moves forward, under the supporting foot.

This thesis proposes a LIPM based reference generation algorithm that uses ZMP references which have not only double support phase but are also more natural since moving ZMP references for single support phase are used. The application of Fourier series approximation simplifies the solution and it generates a smooth ZMP reference. Trajectory and force control methods for locomotion are devised and applied too.

The developed techniques are tested through simulation with a 12 DOF biped robot model. The results obtained are promising for implementations.

ÖZET

İnsansı robotlar geçtiğimiz otuzbeş sene içerisinde pek çok araştırmacının ilgisini çekmiştir. Bu araştırmaların motivasyonu yürüyen robotların insanların yaşadığı ortamlara uygunluğundan ileri gelmektedir. Öte yandan böyle bir sistemin denetlenmesi, sistemin doğrusal olmayan dinamiği nedeniyle büyük zorluk teşkil etmektedir.

Bu doğrultuda yürüyüş referans yörüngesi elde edimi önemli bir çözüm teşkil etmektedir. Böyle bir yörünge eldesi işlemi için gerekli şart elde edilen yörüngenin robotun doğal dinamiği ile takibe uygun olması ve minimum denetleme müdahaleleri ile gerçekleştirilebilmesidir. Inverted Pendulum Model (LIPM) referans yörünge eldesi metoduna dayanan teknikler bahsedilen bu şarta dayanmaktadır. Öte yandan Zero Moment Point (ZMP) kriteri robot yürüyüşünün kararlılık tahlili için geniş çaplı olarak kullanılmaktadır. Dahası, LIPM tabanlı yörünge referansı eldesi modellerin ZMP kriteri ile geliştirilmiş versiyonları da literatürde mevcuttur. Ancak bu metodlarda adım esnasında ZMP çoğunlukla destek ayak tabanının ortasında tutulmuştur. Nitekim böyle bir referans yörünge eldesi doğallıktan uzaktır, çünkü insan yürüyüş çevriminde ZMP ayak tabanı altında sabit kalmaktan ziyade destekleyici ayağın tabanında yürüyüş yönünde ilerlemektedir.

Bu tezde LIPM referans yörünge eldesi metoduna ve destekleyici ayağın altında konumu değişen ZMP referans eğrilerine dayanan bir referans yörünge eldesi metodu ileri sürülmektedir. Fourier serileri yaklaşımı LIPM dinamiğinin çözümünü basitleştirmekle kalmayıp aynı zamanda yumuşak ZMP değişimlerinde olanak sağlamaktadır. Hareket sağlanımı için yörünge ve kuvvet denetleme metodları tertip edilmiş ve uygulanmıştır.

Geliştirilen bu teknikler bir simülasyon ortamında 12 Serbestlik Dereceli bir robot modeli üzerinde denenmiştir. Elde edilen sonuçlar gerçek denemeler için ümit vericidir.

To the loving memory of my grandmother...

ACKNOWLEDGMENTS

First of all, I would like to express my deepest regards and appreciation to Dr.Kemalettin Erbatur for his invaluable support for the realization of my thesis and for his deepest patience to my uncontrollable enthusiasm on new concepts and hastiness.

Also thanks to all Mechatronics graduate students for sharing nights with me in the research lab, supporting me, and especially for their friendship.

And my parents, for their infinite encouragement and moral support...

TABLE of CONTENTS

ABSTRACT.....	iv
ÖZET	v
ACKNOWLEDGMENTS	vii
TABLE of CONTENTS	viii
LIST of TABLES.....	ix
LIST of FIGURES	x
LIST of SYMBOLS.....	xiii
LIST of ABBREVIATIONS	xv
1. INTRODUCTION	1
2. TERMINOLOGY on BIPEDAL WALK	4
3. LITERATURE REVIEW	13
3.1. History of Biped Robotics	13
3.2. Literature Review on Pattern Generation for Bipedal Walking Robots	18
4. REFERENCE GENERATION with NATURAL ZMP TRAJECTORIES.....	27
4.1. Linear Inverted Pendulum Model.....	28
4.2. Natural ZMP Trajectories.....	31
4.3. Exact Solution of Linear Inverted Pendulum Model for Fixed ZMP.....	32
4.4. Planning an Approximate Solution.....	37
4.5. Introduction of Natural ZMP Reference Trajectories by Fourier Approximation to Obtain CoM Trajectories.....	40
4.6. Introducing Double Support Phase to ZMP Reference Trajectories.....	42
5. COORDINATION and CONTROL of LOCOMOTION	46
6. THE BIPED MODEL and SIMULATION RESULTS	60
7. CONCLUSION and FUTURE WORK	68
8. APPENDIX.....	69
REFERENCES	72

LIST of TABLES

Table 6.1.	Masses and dimensions of the biped robot links	61
Table 6.2.	D-H Parameters of the biped leg	61
Table 6.3.	Some of the important simulation parameters	63
Table 6.4	PID Controller Gains for Support Leg Joints	63
Table 6.5	Stiffness Control Gains for Swing Leg Controllers	63

LIST of FIGURES

Figure 2.1	Reference frames for Human Body.....	4
Figure 2.2	Static gait type.....	5
Figure 2.3	Dynamic gait type.....	5
Figure 2.4	The Human Gait Cycle.....	7
Figure 2.5	Gait initiation and termination.....	8
Figure 2.6	Foot steps and CoM trajectory of a human.....	8
Figure 2.7	A person who starts running.....	9
Figure 2.8	(a) Exploded view of the joints and their axes; (b) Joint axes and their placements.....	10
Figure 3.1	All the robots from Honda's Humanoid Project since 1986.....	14
Figure 3.2	Honda's ASIMO.....	14
Figure 3.3	Sony's QRIO.....	15
Figure 3.4	Humanoid Robot Johnnie of the University of Munich.....	16
Figure 3.5	The last prototype of Humanoid Research Project: HRP-2.....	16
Figure 3.6	Honda's P2.....	19
Figure 3.7	An inverted pendulum with constant height.....	21
Figure 3.8	Gravity Compensated Inverted Pendulum.....	23
Figure 3.9	MORPH 3.....	25
Figure 4.1	Some pictures of the used test bed robot, Mari-2.....	28
Figure 4.2	The Table-Cart Model.....	30

Figure 4.3	Kinematic Chain for CoM.....	32
Figure 4.4	A Natural ZMP Trajectory.....	32
Figure 4.5	x -axis ZMP reference trajectory.....	34
Figure 4.6	y -axis ZMP reference trajectory.....	34
Figure 4.7	$p_y^{ref} - p_x^{ref}$ on $x - y$ plane ZMP reference trajectory / Step Positions.....	35
Figure 4.8	$p'_x(t)$ Introduced odd Function.....	38
Figure 4.9	C_x Reference trajectory for x -axis (Saggital Plane).....	39
Figure 4.10	C_y Reference Trajectory for y -axis (Frontal Plane).....	39
Figure 4.11	Natural ZMP reference trajectory.....	40
Figure 4.12	$p'_x(t)$ New introduced odd function.....	41
Figure 4.13	C_x Trajectory with Variable ZMP.....	42
Figure 4.14	Fourier Approximation w/o Lanczos Sigma Factor.....	43
Figure 4.15	Fourier Approximation with Lanczos Sigma Factor.....	43
Figure 4.16	Natural C_x reference with parameters close to human walk.....	45
Figure 4.17	Natural C_y reference with parameters close to human walk.....	45
Figure 5.1	The swing foot position references are obtained from ZMP and CoM references.....	46
Figure 5.2	World frame directions.....	47
Figure 5.3	The ZMP and CoM position reference y -components.....	48
Figure 5.4	The CoM reference y -component in the initialization phase.....	48
Figure 5.5	Robot configurations at the beginning (left) and at the end (right) of the configuration phase.....	49
Figure 5.6	Typical ZMP reference position in the y -direction and swing timing detection.....	50
Figure 5.7	Typical swing foot z -direction position references and their timing with respect to the ZMP references.....	50

Figure 5.8	The ZMP and CoM reference x -components.....	51
Figure 5.9	The ZMP and CoM reference x -components, a closer view.....	52
Figure 5.10	CoM reference and swing foot x -components.....	52
Figure 5.11	CoM reference and swing foot x -components, a closer view.....	53
Figure 5.12	The switching between control modes is realized by processing the ground interaction force and swing foot reference timing.....	54
Figure 5.13	The position references used in different control modes.....	54
Figure 5.14	The robot in the double support phase can be regarded as a trunk manipulated by two six-DOF manipulators based on the ground.....	56
Figure 5.15	The double support phase controller structure.....	56
Figure 5.16	The robot in swing phases can be seen as a ground based manipulator and a second manipulator based at the hip.....	57
Figure 5.17	The single support controller for the right foot.....	58
Figure 5.18	The swing controller for the left foot.....	58
Figure 5.19	The single support controller for the left foot.....	59
Figure 5.20	The swing controller for the right foot.....	59
Figure 6.1	Some pictures of the used test bed robot, Mari-2.....	60
Figure 6.2	A screen shot from the Biped Animation.....	62
Figure 6.3	CoM and CoM reference y -direction components.....	65
Figure 6.4	ZMP and ZMP reference y -direction components.....	65
Figure 6.5	CoM and CoM reference x -direction components.....	66
Figure 6.6	ZMP and ZMP reference x -direction components.....	66
Figure 6.7	CoM and CoM reference on the x - y -plane.....	67
Figure 6.8	ZMP and ZMP reference on the x - y -plane.....	67

LIST of SYMBOLS

A_B	: Base-link attitude matrix
$C(\mathbf{x}, \mathbf{v})$: Centrifugal and Corioli's force matrix
\mathbf{f}_E	: External force vector
$\mathbf{g}(\mathbf{x})$: Gravity vector
$H(\mathbf{x})$: Inertia matrix
K_d	: PID controller derivative gain
K_E	: External force to generalized force transformation matrix
K_i	: PID controller integral gain
K_p	: PID controller proportional gain
\mathbf{p}_B	: Base-link position vector
\mathbf{u}_E	: Generalized force vector generated by external forces
\mathbf{v}	: Generalized velocities vector
\mathbf{v}_B	: Base-link velocity vector
$\dot{\mathbf{v}}_B$: Base-link acceleration vector
$\boldsymbol{\omega}$: Joint angular velocity vector
$\dot{\boldsymbol{\omega}}$: Joint angular acceleration vector
$\boldsymbol{\omega}_B$: Base-link angular velocity vector
$\dot{\boldsymbol{\omega}}_B$: Base-link angular acceleration vector
$\boldsymbol{\theta}$: Joint angle vector
C	: Center coordinates of the Inverted Pendulum
x_{ZMP}	: Zero Moment Point in x-direction
y_{ZMP}	: Zero Moment Point in y-direction

- P : Zero Moment Point reference vector
- z_c : Constant height of the Linear Inverted Pendulum
- ω_n : Square root of $z_c / g(z)$
- τ_{zmp} : Torque generated around the Zero Moment Point
- P_x^{ref} : Reference ZMP for x-direction
- P_y^{ref} : Reference ZMP for y-direction
- A : Foot center to foot center distance in frontal plane
- B : Foot center to foot center distance in sagittal plane
- T_0 : Step Period
- b : Half length of the foot sole

LIST of ABBREVIATIONS

CoM	:	Center of Mass
ZMP	:	Zero Moment Point
LIPM	:	Linear Inverted Pendulum Mode
GCLIPM	:	Gravity Compensated Linear Inverted Pendulum Mode
DOF	:	Degrees of Freedom
m	:	kilogram
s	:	Seconds
LxWxH	:	Length x Width x Height
D-H	:	Denavit-Hartenberg

Chapter 1

1. INTRODUCTION

Humanoid robotics attracted the attention of many researchers in the past 35 years. It is currently one of the most exciting topics in the field of robotics and there are many ongoing projects on this topic [1-7].

The motivation of research is the suitability of the biped structure for tasks in the human environment and the goal of the studies in this area is to reach the human walking dexterity, efficiency, stability, effectiveness and flexibility.

If robots with legged locomotion and wheeled locomotion were to be compared, first, some basis criteria have to be found. The first criterion that comes to mind would be the environment in which the robot will travel. According to this criterion legged robots offer better mobility than their wheeled counterparts. The main reason is that legged robots can use discrete footholds on the ground between which there may exist discontinuities or irregularities while wheeled robots, on the other hand, require a continuous type of landscape, in other words an unbroken path to travel. In fact, human environments generally do contain irregularities, which are not suitable for wheeled robots. In this context, although wheeled locomotion is much more efficient on smooth flat surfaces legged locomotion offers a better mobility and efficiency on irregular ground surfaces. A great proportion of the land animals, especially mammals use legged locomotion. The reason for this fact is probably the efficiency, mobility and adaptability that the legged locomotion brings.

Presumably the best aspect of legged locomotion is its adaptability. Legged locomotion can either apply walking, running or even climbing if necessary. Therefore, it can be concluded that speaking of human oriented environments legged locomotion do offer the best solution.

The hope is to use bipedal robots to complete tasks which are either too difficult or dangerous for humans, such as extreme environmental conditions (fire rescue

operations, space explorations or with explosives such as landmines or radioactive plants). Furthermore, the advantages can be broadened to domestic use such as daily house cleaning or helping elder people. Also, the research provides a good basis for prosthetic devices.

The control of a biped humanoid is a challenging task due to the many degrees of freedom involved and the non-linear and hard to stabilize dynamics.

Walking reference trajectory generation is a key problem. Methods ranging from trial and error to the use of optimization techniques with energy or control effort minimization constraints are applied as solutions.

A very intuitive criterion used for the reference generation is that the reference trajectory should be suitable to be followed by the robot with its natural dynamics, without the use of extensive control intervention. Reference generation techniques with the so-called Linear Inverted Pendulum Model are based on this idea [8]. Simply stated, the walking cycle is then achieved by letting the robot start falling into the walking direction and to switch supporting legs to avoid the complete falling of the robot.

Yet another intuitive demand for the biped robot reference generation is that the reference trajectory should be a stable one, in the sense that it should not lead to unrecoverable falling motion. The Zero Moment Point Criterion [9] introduced to the robotics literature in early 1970s is widely employed in the stability analysis of biped robot walk. Improved versions of the Linear Inverted Pendulum Model based reference generation, obtained by applying the Zero Moment Point Criterion in the design process, are reported too. Generally, in these approaches the Zero Moment Point during a stepping motion is kept fixed in the middle of the supporting foot sole for the stability, while the robot center of mass is following the Linear Inverted Pendulum path.

Although reference generation with the Linear Inverted Pendulum Model and fixed Zero Moment Point reference positions is the technique employed for the most successful biped robots today, this kind of reference generation lacks naturalness at one point. Investigations revealed that the Zero Moment Point in the human walk does not stay fixed under the supporting foot. Rather, it moves forward from the heel to the toe direction [10, 11].

This thesis proposes a reference generation technique based on the Linear Inverted Pendulum Model and moving support foot Zero Moment Point references. With this, an improvement towards the naturalness of the human walk is aimed. The application of

Fourier series approximation to the solutions of the Linear Inverted Pendulum dynamics equations does not only simplify the solution, but it generates a smooth Zero Moment Point reference for the double feet support phase too.

The reference generation techniques mentioned above generate reference trajectories for the center of mass of the robot, the timing of the steps and landing position references for the swung feet. They alone cannot provide swing foot trajectories. Additional foot trajectory generation methods for smooth swing foot trajectories are developed in this thesis too.

Finally, in order to validate the applicability of the generated references their performance has to be tested on walking robot simulations or experiments. However, walking can only result from the harmonious use of suitable reference trajectories and a successful control method. This fact makes the solution of the biped robot control problem as a must to be fulfilled before the reference generation algorithms can be tested. Trajectory control methods for the center of mass of the robot and force control techniques for the landing foot are devised and applied in this thesis too.

The reference generation and control techniques are simulated and animated in a 3-D full dynamics simulation environment with a 12 DOF biped robot model. The results obtained are promising for implementations.

The next Chapter gives an overview of the terminology used in the biped robotics field. Chapter 3 presents a literature survey on successful examples of biped robots, reference generation and control methods. Reference generation with natural moving ZMP trajectories and the control of locomotion are discussed in Chapters 4. Chapter 5 presents the Coordination and Control discussions. The biped model and simulation results are presented in Chapter 6. Finally in Chapter 7 Conclusion and future work is discussed.

Chapter 2

2. TERMINOLOGY on BIPEDAL WALK

Humans are very accomplished bipedal walkers. In fact, human walking represents the most remarkable solution of the nature among the bipedal walking creatures. Therefore it is an advantage to examine the human body structure before taking a step for the design phase of an anthropomorphic walking robot.

An introduction to some terminology used in bipedal research and human biomechanics is presented below. Furthermore some important aspects of human walking process are discussed.

In bipedal research area it is a general approach to use reference frames and terminologies to discuss about set of motions. The reference frames used in this thesis is depicted in Fig. 2.1.

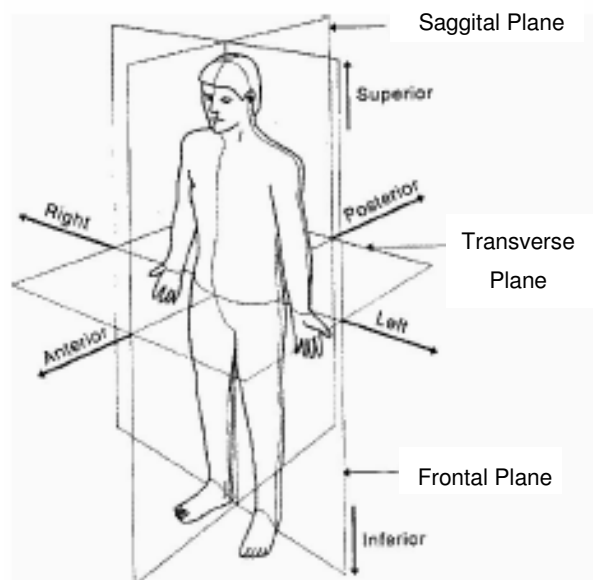


Figure 2.1. Reference frames for Human Body.

Before getting deeper into discussions it is found convenient to start with basic definitions since they are going to be used either in this chapter and the rest of the dissertation frequently. More detailed information can be found in [12].

Center of Mass (CoM): A point at which the whole distributed mass of an object acts.

Supporting Polygon: The polygon shaped over the ground by foot (feet) that is (are) in touch with the ground.

Step length: Distance traveled by one foot

Stride length: Distance traveled between two successive placements of the same foot.

Single Support: The time interval in which only one foot supports the whole body.

Double Support: The time interval in which both feet supports the whole body.

Static Gait: The walking pattern during which the CoM must be over the supporting polygon at all times as shown in Fig. 2.2.

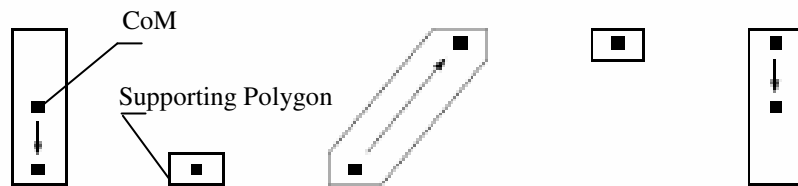


Figure 2.2. Static gait type.

Dynamic Gait: The walking pattern during which there are times when the CoM can be outside the supporting polygon as shown in Fig. 2.3.

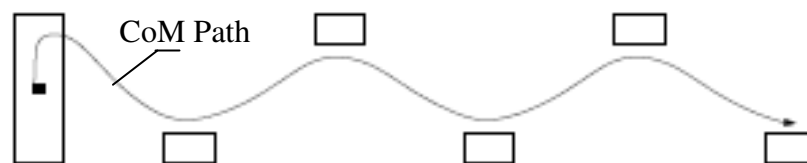


Figure 2.3. Dynamic gait type.

Gait, simply, is defined to be the pattern of footsteps at a particular speed, or a manner of walking or running. This cyclic motion can be broken into two phases: swing and stance (Support) phase. A leg is in its swing phase when it is freely (not touching the ground) moving in the space and it is in its stance phase when it touches the ground or, in other words, exactly when the other leg enters its swing phase. The stance phase can also be broken into two different phases: Single support and Double Support phases. Single support phase is the time interval when only one leg carries the body load. The double support phase, on the other hand, is the time interval when both feet support the whole body. Furthermore, if both feet are off the ground then this phase is called the ballistic phase or the flight phase which actually happens during running.

Gait cycle, for zero initial speed, starts with the double support phase and proceeds. In Fig. 2.4, a typical human walking cycle is depicted. It has been measured that approximately 20% of a typical gait cycle is the double support phase. If this time increases the achievable maximum speed decreases as a result. In fact, running gaits consists of consecutive single support phases only.

The analysis of walking process comprises two key subjects that need to be clarified to get a better insight: The gait cycle and the spatial displacements of the CoM. The displacement of the center of mass is a key concept in walking cycle due to the fact that it hosts the definition of stability in a sense. In other words, it can be regarded as a basis to understand stability in any type of gait.

Static and dynamic locomotion are the two types of walking that are distinguished by the location of the center of mass in the gait cycle. In static walking the vertical projection of the center of mass of the robot lies inside the supporting polygon created by the foot/feet of the robot at all times (Fig. 2.2). Hence at any time the robot is statically stable or, in other words, if the gait cycle is paused at any time during the walk the robot wouldn't fall down eventually. On the other hand, in dynamic walking the vertical projection of the center of mass can lie outside the supporting polygon sometimes (Fig. 2.3). Although this is an indication of instability, the overall gait is kept dynamically stable due to the inertial effects. In other words, a dynamically stable gait cycle contains local controlled instability regions in such a way that the overall stability is preserved. Thus this fact, eventually, brings the challenge to generate dynamically stable reference gaits in humanoid robotics. Although it is the case, actually, this challenge comes with a prize that does not exist in the static walking: speed. By the

correct regulation of speed the stability of the gait cycle is achieved. In fact, human walking patterns are considered to be dynamically stable in which there are consecutive fallings from one foot to the next.

Generally static gait is slow by its nature. The reason for this fact is that in static gaits CoM has to lie within the region of the supporting polygon always. However, in dynamic gaits the opposite of this fact holds. Since the CoM spends less time within the supporting polygon higher speeds are achieved, in fact, dynamic walk becomes extremely hard to realize if the speed of the gait is too slow. Because at slow speeds the time spent in which the CoM lies outside the supporting polygon increases and hence the effect of gravity becomes more dramatic. Therefore the probability of falling down increases eventually.

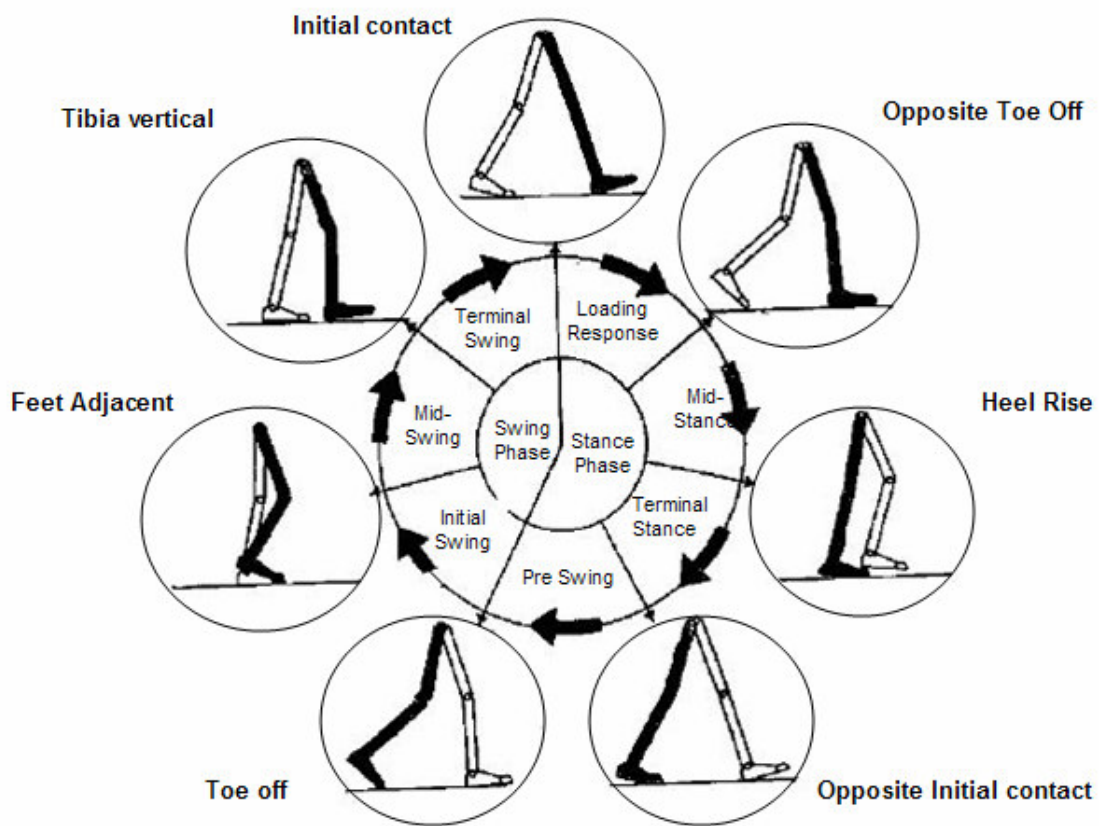


Figure 2.4. The human gait cycle [13].

These facts can also be seen in the following figures from human walking data. For the cases of gait initiation and gait termination CoM path is depicted in Fig. 2.5.

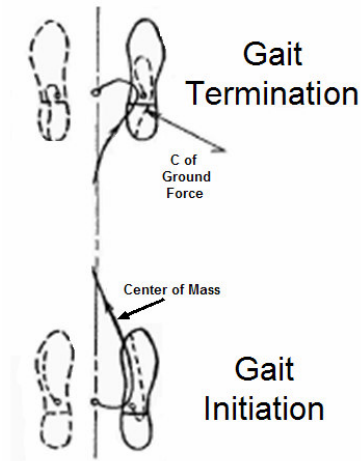


Figure 2.5. Gait initiation and termination [13].

Note that during the gait initiation and the gait termination the body speed is relatively slow, and hence CoM is inside the supporting polygon during this time.

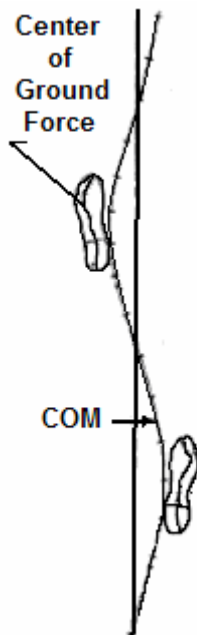


Figure 2.6. Foot steps and CoM trajectory of a human [13].

To point out the stability of the walk it is interesting to notice that during steady walk (at constant speed), the CoM trajectory does not run out of the supporting polygon, Fig. 2.6. In fact, the result of such a change would be falling. The reason behind dynamically stable walk is that either there are enough forces and moments generated to oppose the gravitational force to prevent the body from falling down, or the time for

single support phase is adjusted in such a way that it is not enough for the gravitational forces to lead for a tipping over. These two factors are often used in synthesizing or generating gaits for bipedal walking machines.

Zero Moment Point (ZMP): The point, generally on the ground surface, around which the total applied torque is equal to zero. It is defined by Vukobratovic, M. [9] and it serves as a stability criterion for the dynamics of multi-body objects.

ZMP can be regarded as a very important tool in reference gait generation for humanoid robotics. Therefore, it is crucial to have a good insight on what it is. The best way to understand ZMP and ZMP based stability would be to consider ourselves, in other words, how we react in certain postures. For instance, in Fig. 2.7, a human athlete in a running posture can be seen. In such a body posture, it is evident that if the person does not accelerate his body forward then, eventually, he will fall down. On the contrary, if he accelerates forward, then for some amount of time he can stabilize his body and keep his balance. In such a case the ZMP, which lies on the ground will be under the supporting polygon (the left foot in this case).

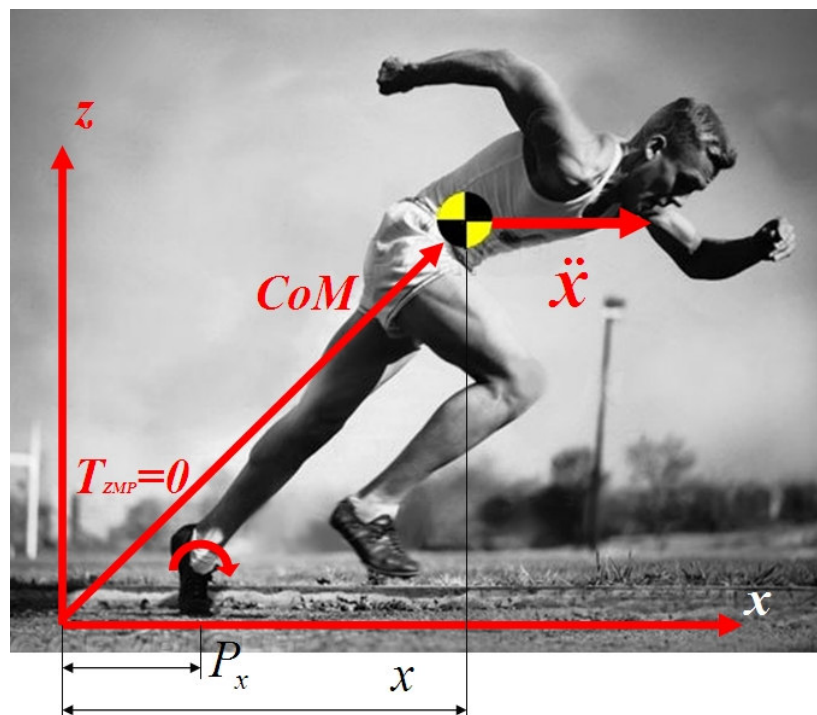


Figure 2.7. A Person Who Starts Running.

Where $P = [p_x, p_y, p_z]^T$ is the ZMP vector, and $CoM = [x, y, z]^T$ is the center of mass vector of the athlete.

In any type of gait it can be concluded that if the ZMP is inside the supporting polygon at all times then the gait is considered to be stable. Note that this definition encapsulates both statically and dynamically stable walking. Since the net applied torque around the ZMP is zero then the tipping moment eventually becomes zero, which means that there is no tipping moment acting on the body. On the other hand if ZMP is outside the supporting polygon then the net torque acting on the body is not zero, and as a matter of fact there exists a tipping moment acting on the body. Hence the gait is not stable and the body may fall down eventually, which is exactly what happens if the person does not accelerate forward in the previous example.

Denavit-Hartenberg Axis Assignment: This is a common axis assignment convention which was originated by Denavit and Hartenberg [14]. The joint axis assignment with the Denavit-Hartenberg convention in [14] is shown in Fig. 2.8.

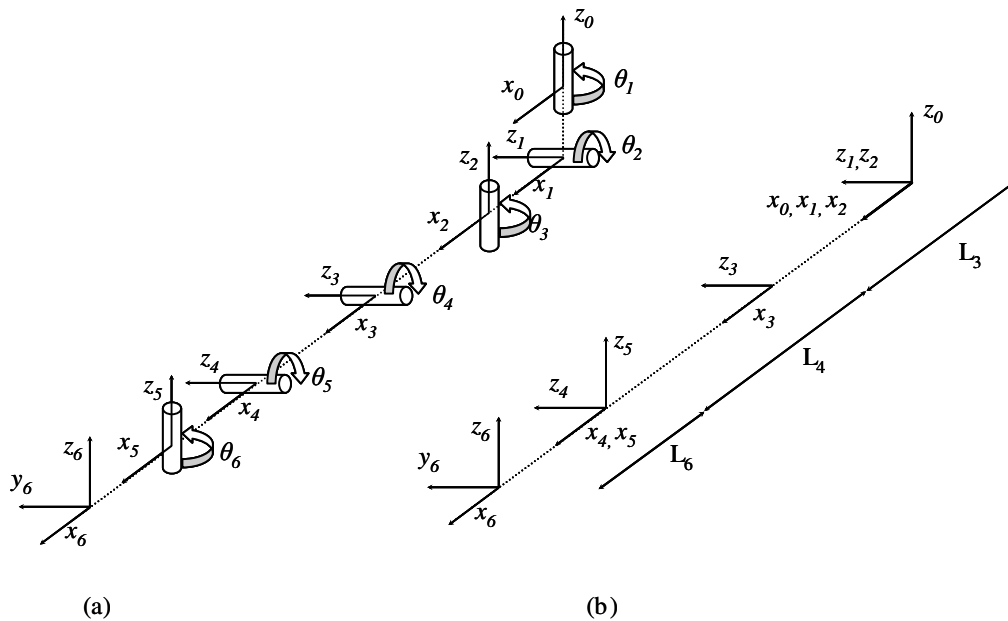


Figure 2.8. (a) Exploded view of the joints and their axes; (b) Joint axes and their placements.

Newton-Euler Dynamic Model: This is a recursive kind of algorithm to model the dynamics of a rigid-body object. Due to its recursive nature it is suitable for online calculation and it is a quite common method to model the dynamics in robotics [14].

Euler-Lagrange Dynamic Model: This is another method of deriving the dynamic model of a rigid-body object which gives closed form equations. This method is also common in robotics and it is again used in online calculation [14].

Tree Structure: It is the kinematic chain structure type used to define two legs of a bipedal walking robot.

Biped Dynamic Model: The biped robot is modeled as a free-fall manipulator which is not fixed to the ground but has interaction with it. In order to formulate the dynamics of a free-fall manipulator, position and attitude variables of the base-link should be introduced. Let generalized coordinates \mathbf{x} , generalized velocities \mathbf{v} , and generalized forces \mathbf{u} be:

$$\mathbf{x}^T = [\mathbf{p}_B^T, \mathbf{A}_B^T, \boldsymbol{\theta}^T] \in R^3 \times SO(3) \times R^N \quad (2.1)$$

$$\mathbf{v}^T = [\mathbf{v}_B^T, \mathbf{w}_B^T, \mathbf{w}^T] \in R^3 \times R^3 \times R^N \quad (2.2)$$

$$\mathbf{u}^T = [\mathbf{f}_B^T, \mathbf{n}_B^T, \boldsymbol{\tau}^T] \in R^3 \times R^3 \times R^N \quad (2.3)$$

where

\mathbf{p}_B : 3×1 vector specifying base-link position

\mathbf{A}_B : 3×3 rotation matrix specifying base-link orientation with respect to a world frame

$\boldsymbol{\theta}$: $N \times 1$ vector specifying joint angle

\mathbf{v}_B : 3×1 vector specifying base-link velocity

\mathbf{w}_B : 3×1 vector specifying angular velocity of base-link

\mathbf{w} : $N \times 1$ vector specifying joint angular velocity

\mathbf{f}_B : 3×1 force vector generated in base-link

\mathbf{n}_B : 3×1 torque vector generated in base-link

$\boldsymbol{\tau}$: $N \times 1$ torque vector generated by actuator

N : Number of joints of the robot

The equation of motion of the robot is:

$$\mathbf{H}(\mathbf{x})\dot{\mathbf{v}} + \mathbf{C}(\mathbf{x}, \mathbf{v})\mathbf{v} + \mathbf{g}(\mathbf{x}) = \mathbf{u} + \mathbf{u}_E \quad (2.4)$$

where

$\mathbf{H}(\mathbf{x})$: $(N+6) \times (N+6)$ inertia matrix

$\mathbf{C}(\mathbf{x}, \mathbf{v})$: $(N+6) \times (N+6)$ matrix specifying centrifugal and Corioli's effects

$\mathbf{g}(\mathbf{x})$: $(N+6) \times 1$ vector specifying gravity effect

\mathbf{u}_E : $(N+6) \times 1$ vector specifying generalized forces generated by external forces

Chapter 3

3. LITERATURE REVIEW

3.1. History of Biped Robotics

The first recorded design of a humanoid robot was made by Leonardo da Vinci in 1495. The robot is a knight, clad in German-Italian medieval armor, which is apparently able to make several human-like motions. These motions include standing up, moving its arms, neck and an anatomically correct jaw. It is partially the fruit of Leonardo's anatomical research in the Canon of Proportions as described in the Vitruvian man¹. This fact was rediscovered from Leonardo's notebooks in the 1950s.

In the 20th century the first computer controlled humanoid robot was designed and built at the Waseda University in 1967, which was called Wabot-1 [15]. At that time the technology of the robot was very impressive. The robot had a stable gait (it took 45 seconds for the robot to take a step) as well as gripping hands with tactile sensors, and a vision system and a communication system. The realization of this first humanoid robot influenced lots of engineers and scientists around the world to orient their research to this subject.

Afterwards, many other bipedal walking robots were developed in the 1980s like WHL-11 of Waseda, which was capable of static bipedal walking on a flat surface at 13 seconds per step speed [16], or like Batelle's Pacific Northwest Laboratories' Manny [17]. Another interesting example of legged locomotion would be M. H. Raibert's

¹**Vitruvian Man:** The Vitruvian Man is a famous drawing with accompanying notes by Leonardo da Vinci made around the year 1490 in one of his journals. It depicts a naked male figure in two superimposed positions with his arms apart and simultaneously inscribed in a circle and square. Vitruvian Man is also referred as the "Canon of Proportions" or "The Proportions of Man".

hopping machine [18] which introduced the ballistic flight phase to bipedal locomotion and demonstrated that the stability can be achieved by bouncing continuously.

However, the ultimate turning point of the history of humanoid robotics would be the time when Honda announced its already existing project on humanoid walking robots (Fig.3.1). The years of experience on many trial and errors led Honda to its ultimate walking robot ASIMO [3]. ASIMO not only has the ability to walk dynamically and naturally but also it has many other features like dexterous manipulation of objects, posture, sound, gesture and face recognition abilities (Fig.3.2).



Figure 3.1. All the robots from Honda's humanoid project since 1986.



Figure 3.2. Honda's ASIMO.

Not long after Honda's success, Sony introduced QRIO in 2004 [4, 5]. This robot also has a dynamically stable walk, and it is capable of adapting to uneven ground surface, detect obstacles and avoid them, recognize face, sound, words, even can have dialogs with people (Fig. 3.3).



Figure 3.3. Sony's QRIO.

Expanding the examples further, University of Munich's JOHNNIE is another bipedal robot that has a dynamically stable gait; the robot is able to walk on even and uneven ground and around curves. Furthermore, a jogging motion is planned for the robot. This is characterized by short ballistic phases where both feet are off the ground. The robot is autonomous in terms of actuators, sensors and computational power, just the energy is supplied by a cable [6]. The robot is able to achieve a dynamic gait and it can also walk up to 2.6 km/h. Also it has a vision system and arms to improve its stability (Fig. 3.4).

Another remarkable example would be the HRP-2 by the Manufacturing Science and Technology Centre (MSTC), which is sponsored by the Ministry of Economy, Trade and Industry (METI), Japan. The robot has 30 degrees of freedom. The cantilevered crotch joint allows for walking in a confined area. Its highly compact electrical system packaging allows it to forgo the commonly used "backpack" used on other humanoid robots [7]. This robot also can achieve a dynamically stable gait; also it can lie down and get up, and carry objects together with people (Fig. 3.5).



Figure 3.4. Humanoid robot Johnnie of the University of Munich.

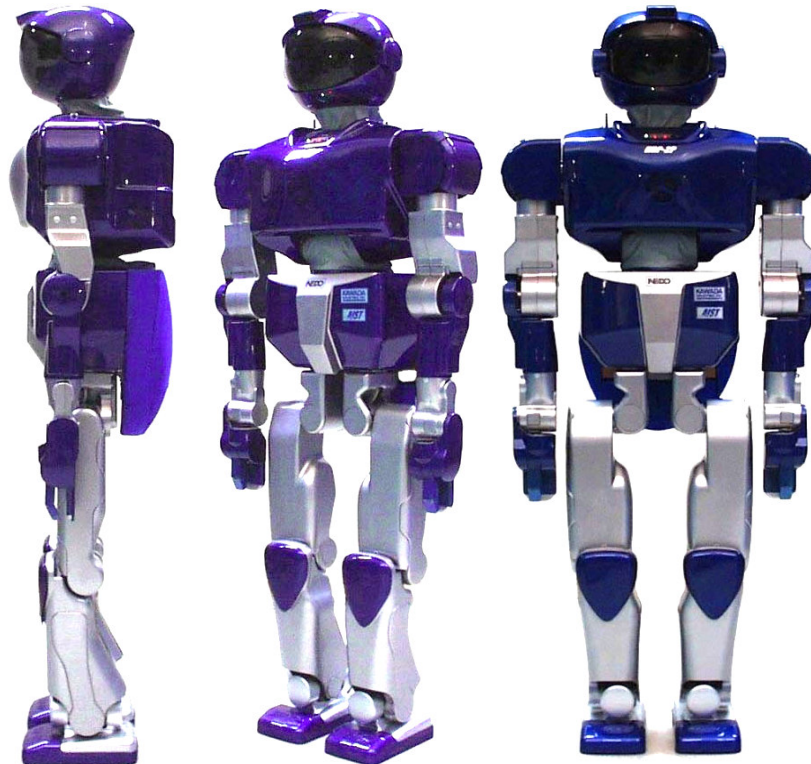


Figure 3.5. The last prototype of Humanoid Research Project: HRP-2.

There are many humanoid projects that continue around the globe, although the trend inclines to eastern countries, like Korea or Japan. And it is natural to expect that humanoid technology will grow faster in proportion with the goal to develop more human-like robots, computer, actuator and sensor technology and, in a sense, help us to understand what it means to be human.

3.2. Literature Review on Pattern Generation for Bipedal Walking Robots

Presumably in the future humanoid robots will be a new form of computer that acts and supports our daily activities in our environment. The reason behind this speculation lies in the nature of bipedal walking which has supreme characteristics in obstacle avoidance when compared with wheeled and multi-legged robots. However, the biped robot dynamics are highly nonlinear, complex and unstable by its nature. This eventually makes biped walking control a highly challenging task. Although there exist many successful accomplishments on bipedal walking and gait generation around the globe, this progress still lacks in many ways when compared to human walking in terms of flexibility, naturalness, stability and robustness. In this context bipedal walking robot research can be considered to be in its initial phases.

There are many different approaches to form a solution to these expectations in literature. These approaches can be classified into two major categories.

The first approach uses precise knowledge of dynamic parameters of a robot e.g. mass, location of mass and inertia of each link to prepare walking patterns. Furthermore, in this approach joint motion trajectory is prepared in advance and it is applied to the real robot with a little online modification. Now let's have a closer and deeper look at some of the existing robot projects falling into this category.

Presumably the most outstanding instance would be Honda's P2 [1], shown in Fig. 3.6. They divided the walking control into three sub-control routines. These routines are Ground Reaction Force Control which shifts the actual ZMP point to an appropriate position by adjusting each foot's desired position and orientation, Model ZMP Control which is used to control the shifting of the desired ZMP to an appropriate position in order to recover the robot posture, and lastly the Foot Landing Position Control which corrects the relative position of the upper body and the feet in conjunction with the model ZMP control. Simply this control scheme corrects the changing geometric arrangement due to possible accelerations of the upper body caused by other sub-control schemes.



Figure 3.6. Honda's P2.

By having these three control routines working simultaneously Honda achieved a posture stabilizing control similar to a human with P2 (Fig.3.6).

Furthermore, it is interesting to notice the lessons that Honda learned after many experiments they developed over walking robots they designed and implemented in their laboratories. After the walking experiments on robots with varying speed and payload, it was concluded that the robot system requires a body inclination sensor, and a ground interaction force sensor for each foot. And also it was seen that to absorb the landing-impact ground reaction force an impact absorption mechanism was required. Additionally to design the shape and dimensions of the robot Honda engineers considered the environment that the robot will work in. For instance the height and the width of the robot is designed for it to be able to fit through a door easily. Its fingers were designed to hold simple objects easily. Furthermore, the angle variations of the joints were kept sufficient enough for the robot to be able to work efficiently and climb average size stairs. Harmonic gear drives and dc motors are used for joints.

Defining constraints on the movement of joints and using iterative computation is another technique used in [19] by Kaneko, K. et. al. They use a method where they generate hip and foot trajectories to determine the rest of the joint trajectories to

generate a walking gait. First they formulate the constraints of a foot trajectory and generate this trajectory by a 3rd order spline interpolation. Or in other words they decide on the points where each foot will be at certain times and use interpolation to fit a curve that includes those points in the working space of the leg. Afterwards, they formulate a hip trajectory using 3rd order periodic spline functions, and derive the hip trajectory with high stability by means of an iterative ZMP calculation. Namely, a hip trajectory is defined according to a given leg trajectory by means of satisfying the ZMP criterion such that the reference ZMP should always lie inside the supporting polygon at all times.

Another interesting approach is in [20] where the authors use kernel of arbitrary stepping motions designed a priori to generate desired dynamically stable motions. The stepping motion to an arbitrary position is done in two stages. The first stage is the construction of kernel motions by means of genetic algorithm. The second is the real-time mixture of pre-designed motions to generate a desired dynamically stable stepping motion.

In [21] a more global approach is taken. The authors consider the robot as a whole when modeling it and generate trajectories for not only its hip and feet but also for its waist joints and arms as well. With this technique they are able to generate a dynamically stable gait.

With the above mentioned approaches, researchers are able to generate dynamically stable gaits. However, as mentioned before these solutions mainly rely on the precise knowledge of the parameters of the humanoid robot being used, moreover there are strict assumptions that may, in fact, lead to possible failures in real life experiments when they are changed, such as the slope of the ground or the weight of the robot. In other words, the method used in these solutions leads them to be inflexible and cumbersome. Instead a humanoid robot must be adaptive and robust to changing parameters in its environment. We believe that the second approach provides a better potential for such an aim.

The second approach uses the limited knowledge of dynamics e.g. location of total angular momentum, total center of mass etc. Since the controller knows little about the system this approach mainly relies on a feedback control.

One of the most effective and hence popular techniques belonging to this group is the linear inverted pendulum mode approach which was introduced by Kajita, S. and

Tani, K. in [22]. In this approach authors aim to extract a dominant feature of biped dynamics and simplify its' non-linear and high-order dynamics by only considering this dominant feature. We believe that their intuition lies in the fact that the dynamics governing the actual human walking sometimes behaves like the dynamics of a falling pendulum at certain times. In this context the authors derive the equations that are governing the dynamics of an inverted pendulum. But these equations were also non-linear and hard to solve. To have linear equations they eliminate the vertical movement by fixing the height of the pendulum. When the motion of a 3D inverted pendulum is constrained to move on an arbitrary plane the dynamics governing the pendulum becomes linear and this, eventually, uncouples the motion to saggital and frontal planes. And they realize that these linear equations are not only easy to manipulate but they are also more or less sufficient enough to describe the actual dynamics of a walking robot. Such an inverted pendulum is shown in Fig. (3.7).

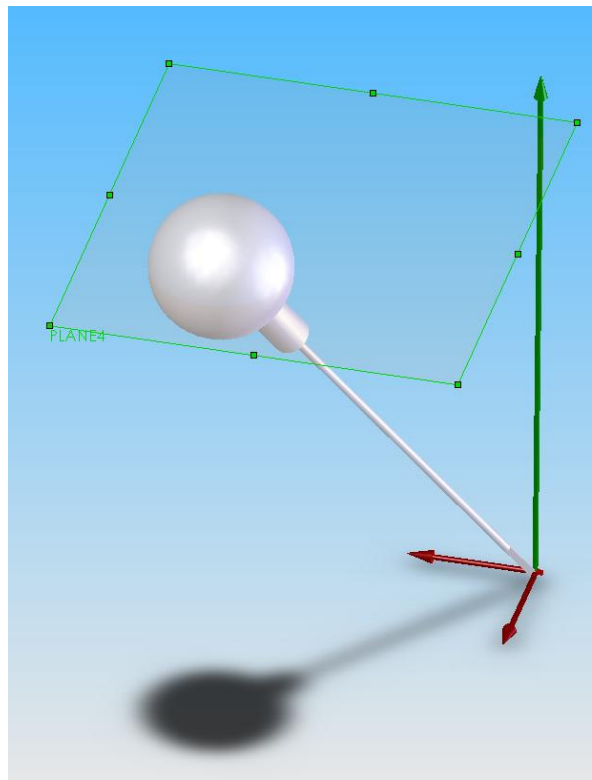


Figure 3.7. An inverted pendulum with constant height.

This method is being used by many researchers around the world [6, 7] since it provides a practical and relatively easy solution which allows for real-time computation of dynamically stable bipedal walking gait.

Looking for a dominant index which will be able to represent the whole system idea is apparently not restricted with the linear inverted pendulum mode approach. In [23] Sono, A. and Furusho, A. aim to develop a control method which allows the robot to walk in a natural manner without resisting the field of gravity. As a quantity to represent the whole state of the system they select the angular momentum and they support their choice by the law of the conservation of the total angular momentum. While employing angular momentum index for the control in the saggital plane they regard the motion in the frontal plane to be an ordinary regulator problem with two equilibrium states. Furthermore, they test their proposed method on their robot BLR-G2 and achieve a walking speed of 0.35cm/sec.

Couple of years after Kajita, S. and Tani, K. introduced the linear inverted pendulum model Park, J.H. et. al came up with the Gravity-Compensated linear inverted pendulum approach [24]. Their intuition stems from the assumption in linear inverted pendulum mode approach that the robot has legs with zero mass. They claim that this assumption, in fact, leads the swinging of each leg to act as a disturbance to the 3D LIPM model. Experiments show that the heavier the legs are when compared to the trunk the higher the disturbance becomes. This was because the inertia effects of those robots which were not negligible. As a solution to this problem, Park, J.H. et. al model the inverted pendulum to be composes of two different masses one of which represents the swinging leg and the other the rest of the body, which can be seen in Fig. 3.8. Having a defined trajectory for the swinging leg they calculate the resulting acceleration and hence the moment effect of the swinging leg and add it to the existing inverted pendulum model after some simplification assumptions. The resulting model actually is nothing but the linear inverted pendulum model when the swinging leg effect is equal to zero. Moreover they design a servo controller for both the swinging leg and center of gravity. Their simulation results indeed show that the swinging leg affects the trajectory of the center of mass dramatically when the mass of the swinging leg is increased.

As an implementation for their previously mentioned idea, Kajita, S. et. al [25] developed a new bipedal walking machine with telescopic legs which were driven by brushless DC servomotors and ball screws. In their studies they develop a solution to

the differential equations, which govern the dynamics of the bipedal robot, in terms of the initial position and velocity. Furthermore, from this solution they derive equations which give the correlation between the cycle and the geometry of the stepping motion

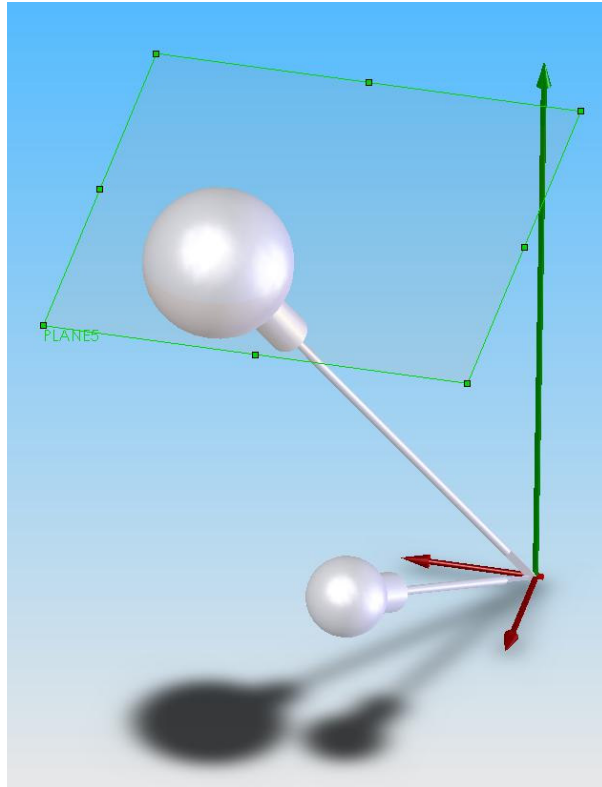


Figure 3.8. Gravity compensated inverted pendulum.

that helps to get an intuition on how the model parameters affect each other. Additionally they develop a double support phase to cope with the disturbances due to leg exchanges. In this implementation Kajita et. al were able to generate trajectories in real-time.

In later approaches it can be observed that the zero moment point stability criterion is starting to come in to the picture by the linear inverted pendulum mode based models. In [26] Inoue, H. et. al develop a real-time motion generation method which controls the center of gravity by indirect manipulation of the ZMP. The indirect term here refers to the fact that ZMP is a resulting value of the system's dynamics which therefore can not be controlled directly. The origin of their idea lies in the dynamical relationship between the ZMP and the center of gravity. Again they assume the legged system to have similar dynamics to the inverted pendulum, whose supporting

point is located at the ZMP point lying on the ground. Thereafter they propose the method that controls the COG of the whole humanoid body in real-time through ZMP manipulation. They use simple linear inverted pendulum equations to derive the strict referential COG trajectory. Although the approach is pragmatic in the sense that it assumes the inertial forces other than the gravitation are zero, they claim that its effectiveness was remarkable. Lastly they decompose the referential COG velocity to joints and apply local controllers for each joint actuator to generate the whole-body motion of the robot.

Although the ZMPs position can be controlled indirectly by giving acceleration references to center of body of the robot this , eventually, will lead to the necessity of modification of the walking pattern designed a priori. But this may not be desirable because the landing points of the free leg will be altered and may touch the ground at undesirable positions. However, these positions are generally determined by the exogenous environmental needs. Kajita, S. et. al brings a solution to this problem in [27]. They handle the problem as follows: ZMP should always lie inside the supporting polygon in order the robot to be stable. Thus any given ZMP trajectory must also define the foot stepping positions. And these ZMP trajectories must be somehow obtained as a result of a suitable biped gait. The core of their solution to the problem is the preview controller that uses the future information of the reference ZMP trajectories in order to control the acceleration of the CoM. Then the resulting (measured) ZMP of the moving CoM fed back to the control loop. Thus, in a sense, the ZMP is controlled indirectly by means of CoM motions and the reference ZMP is tracked. Finally they use the obtained CoM trajectory with the foot stepping positions obtained from the given ZMP trajectories as references for the actual robot.

Another approach was developed by Okumura, Y. et. al to the same problem in [28]. What they propose is such an algorithm that preserves the pre-assigned landing positions of the swinging leg. Their approach to achieve this result is as follows; The spatial trajectory of a joint in 3D is traversed at different speeds depending on the necessary acceleration to stabilize the gait according to the ZMP formulas. And the difference in speed is nothing but the difference in sampling time. Hence, by varying the sampling time they can achieve different accelerations. Thus, the acceleration required for ZMP compensation can be exerted without disturbing the pre-computed spatial leg trajectory. In other words they are able to keep the pre-specified stepping positions

while they stabilize the robots gait dynamically. Furthermore, they test this algorithm on the robot “Morph3” which was created at their laboratories, Fig. (3.9).

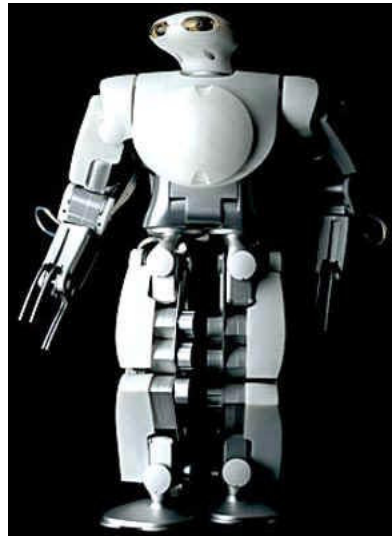


Figure 3.9. MORPH 3.

Although the linear inverted pendulum approach provides both a simple and real-time computable solution, another drawback of this method is that the governing equations are unstable. Of course this is a natural outcome since an inverted pendulum is unstable itself. In [29] Choi, Y. and his co-workers derive equations for the center of gravity of the robot which they assume to be a rolling sphere on a virtual arbitrary plane with the height of the robot’s COG from the ground. Later by introducing the ZMP definitions to these equations they derive the ZMP equations in the state space and get the exact solution by using reference ZMP curves which also define the footstep positions in time. However, they claim that the solution is not robustly applicable for real biped walking system since they are composed of unbounded $\cosh(.)$ functions, and that those solutions happen to be very sensitive to the variation of the height of the COG. As a solution to this matter they plan an approximate solution composed of bounded cosine and sine functions by means of Fourier series. Lastly they come up with approximated simple bounded functions to serve for COF trajectory which also satisfies the reference ZMP curves. Lastly, to cope with the possible disturbances in the real implementation they develop an indirect control for the ZMP.

In gait planning and control of biped walking, most of the above mentioned methods use fixed ZMP references. In other words, they assume discrete points for ZMP reference which are actually in the middle of the sole of the foot. On the other hand, in human walk ZMP does not just stay fixed at a point but it travels on the ground as the gait cycle proceeds. In [30] Kawamura et. al proposes this idea of using variable ZMP to generate a dynamically stable gait in terms of linear inverted pendulum approach. Their claim is that using a fixed ZMP not only leads to the biped walking rigid but also leads the walking to lack of flexibility. So in order to make the biped walking more human like and more agile it is necessary and important to investigate the biped walking with variable ZMP. They use 3rd order spline curves for ZMP references and consider it to move from the heel to toe of the foot in single support phase by line functions. Furthermore they investigate the stable biped walking condition from ZMP concept, frictional constraint, and inverted pendulum model. Lastly they compare the aspects of fixed and variable ZMP according to their simulation results.

Chapter 4

4. REFERENCE GENERATION with NATURAL ZMP TRAJECTORIES

LIPM mode approach is based on such ordinary differential equations that the solutions are both hard to be solved and they are composed of numerically unbounded $\cosh(.)$ functions. In addition they are sensitive to the height variation of the pendulum and they are difficult to be used robustly. Furthermore, since only the acceleration of the body is considered in LIPM approach the foot stepping positions may vary as a result. However, the stepping positions in real implementations are generally determined by exogenous environmental needs. For instance a robot should determine its foot stepping positions in order to avoid obstacles in real experiments. As a result the robot should have such a gait that follows the pre-determined stepping positions and preserve the overall stability.

As a solution to such problems Choi, Y. et. al [29] introduce an alternative robust CoM trajectory planning method by using the approximate solution composed of bounded functions. Having pre-determined ZMP reference trajectories Choi, Y. et. al find the exact solutions of LIPM equations that are derived according to ZMP criterion. Finally they derive the approximated closed form equations that give the time trajectory of the CoM.

However in their studies Choi, Y. et. al use fixed ZMP trajectories. This actually leads the robot walking both to be rigid and unnatural. Furthermore, in their approximated solutions they do not consider double support phases which, eventually, may bring problems in real implementations [6,30].

In this chapter the approximation to the solution of the dynamics of LIPM, which is done by Choi, Y. et. al, is shown and the main contribution of this thesis, that is, the introduction of Natural ZMP references with double support phase to this method is discussed.

4.1. Linear Inverted Pendulum Model

Linear Inverted Pendulum Model was first introduced by Kajita and Tani in 1991 [22]. The main idea of this approach is to extract a dominant feature of biped dynamics, which is high-order and non-linear, and to use this dominant factor to explain the governing dynamics of the system. In this model the robots mass is assumed to be lumped at the center of mass of the robot and the legs of the robot are assumed to be massless. Further, for simplicity, the height of the pendulum is assumed to be constant in this model. This lets the dynamics of the model to be linear. Such an inverted pendulum with a massless rod can be seen in Fig. 4.1.

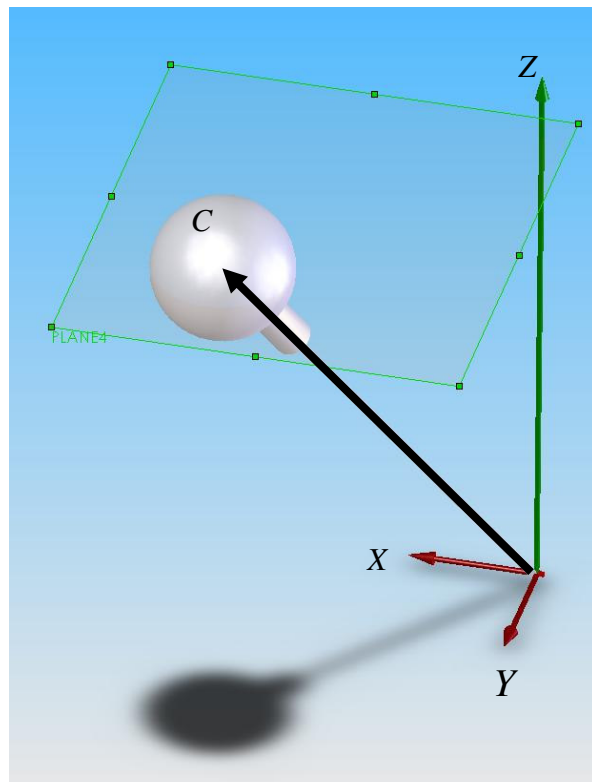


Figure 4.1. Inverted pendulum.

where $C = [c_x, c_y, c_z]^T$.

The ZMP equations for $x - y$ plane are as follows.

$$x_{zmp} = \frac{\sum_{i=1}^n m_i (\ddot{z}_i - g_z) x_i - \sum_{i=1}^n m_i (\ddot{x}_i - g_x) z_i}{\sum_{i=1}^n m_i (\ddot{z}_i - g_z)} \quad (4.1)$$

$$y_{zmp} = \frac{\sum_{i=1}^n m_i (\ddot{z}_i - g_z) y_i - \sum_{i=1}^n m_i (\ddot{y}_i - g_y) z_i}{\sum_{i=1}^n m_i (\ddot{z}_i - g_z)} \quad (4.2)$$

Where, $P_{ZMP} = [x_{zmp}, y_{zmp}, z_{zmp}]^T$ shows the ZMP vector of any kinematic chain, the gravity vector is $g = [g_x, g_y, g_z]^T$ and $g_z = -g$, $[x_i, y_i, z_i]^T$ and m_i is the position vector and the mass of each link, respectively.

Now, let the ZMP of coordinates of this pendulum to be $P = [p_x, p_y, p_z]^T$, the mass of the pendulum to be m . The gravity vector is $g = [g_x, g_y, g_z]^T$, $g_z = -g$, and $C = [c_x, c_y, c_z]^T$ is the CoM vector. Using the ZMP equations (4.1) and (4.2) the dynamics equations of the inverted pendulum can be derived as follows.

$$p_x = \frac{m(\ddot{c}_z + g)c_x - m\ddot{c}_x c_z}{m(\ddot{c}_z + g)} \quad (4.3)$$

$$p_y = \frac{m(\ddot{c}_z + g)c_y - m\ddot{c}_y c_z}{m(\ddot{c}_z + g)} \quad (4.4)$$

However equations (4.3) and (4.4) are non-linear. To attain linear equations assume the z-coordinates of the inverted pendulum is assumed to be constant. Let $c_z = z_c$. Thus the equations (4.3) and (4.4) turn into linear equations as follows.

$$p_x = c_x - \frac{1}{\omega_n^2} \ddot{c}_x \quad (4.5)$$

$$p_y = c_y - \frac{1}{\omega_n^2} \ddot{c}_y \quad (4.6)$$

where $\omega_n^2 = \frac{g}{z_c}$.

Henceforth, (4.5) and (4.6) are going to be referred as ZMP equations. Note that given the CoM coordinates of the pendulum $C = [c_x, c_y, c_z]^T$ at any time it is straightforward to calculate the ZMP coordinates of the pendulum by (4.5) and (4.6). On the other hand walking trajectory generation is the inverse problem. That is, given a ZMP trajectory a CoM trajectory should be found. Thus, this trajectory of CoM could be used as a reference for the CoM of the actual biped walking robot. Further the legs should be in such coordination that this CoM is tracked accurately. Since the goal is to achieve a dynamically stable gait the ZMP trajectory should always lie inside the supporting polygon. And this actually determines the location of the footprints of the biped robot. Finally by knowing the footprints and the CoM trajectory by inverse kinematics relations a possible gait could be achieved.

A good example in order to have a better insight and intuition on LIPM model is the Table-Cart model which is used by Kajita in [27]. Such a Table-Cart model can be seen in Fig. 4.2. Actually the governing dynamics of the LIPM is exactly analogous to the Table-Cart model since the height of the pendulum is assumed to be constant.

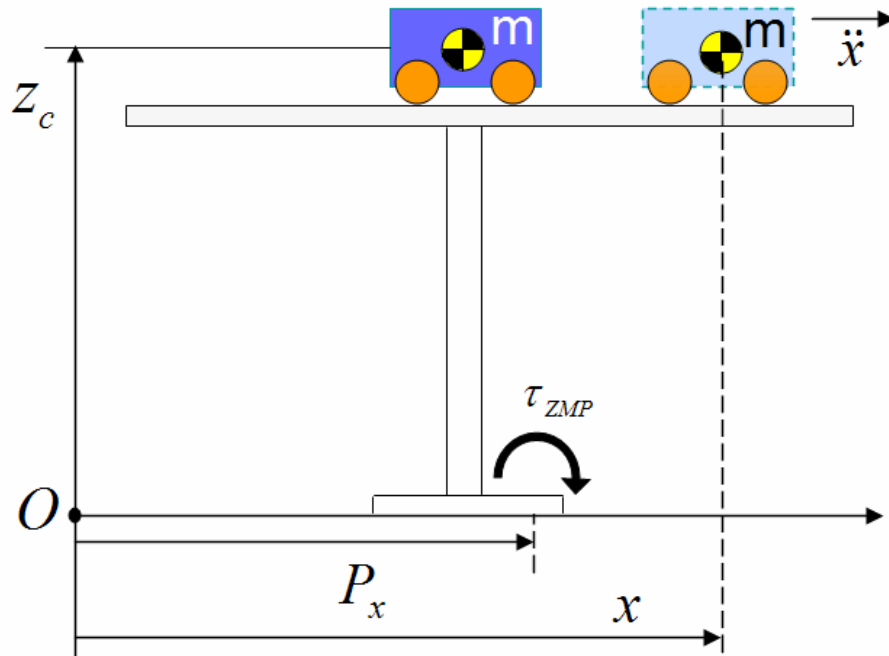


Figure 4.2. The Table-Cart model.

As depicted in the picture, assume the cart to be at the position showed by dashed lines. If the cart is not moving then, since the foot of the table is not long enough to equalize the torque generated by the cart, the table would fall eventually. However, if the cart has a proper acceleration, the table can remain upright for a while. At the moment, ZMP lies inside the table foot. Notice that this example is similar to the one which is given in Chapter 2 (Fig. 2.7). Since the moment around the ZMP must be zero the following condition holds.

$$\tau_{ZMP} = mg(x - p_x) - m\ddot{x}z_c = 0 \quad (4.7)$$

A similar Cart-Table model can also be considered for the y-axis, and same result can be obtained from (4.1).

4.2. Natural ZMP Trajectories

Bipedal walking robots are instable structures by their nature and can tip over easily. Since biped robots are unactuated at the base link these stability problems emerge eventually and bring the challenging problems of gait generation and control of biped robots for dynamically stable walking into front. A commonly known concept that serves as a stability criterion for biped robot systems is the so-called ZMP, which was originally introduced by Vukobratovic, M. [9].

A kinematic chain is depicted in Fig. 4.3. The ZMP for such a system can either be measured by means of force sensors or it can be computed. The ZMP of the robot should be always in the supporting polygon for it to be in a stable condition. This implies that the robot is continuously recovering from unbalanced conditions to a stable posture. Stable ZMP references can be employed to design stable walking patterns.

Usually in many reported studies [26-29], the ZMP reference in the single foot support phase is in the form of a point under the sole of the supporting foot. However, experiments with walking humans show that the ZMP does not stay at a fixed point in

the single support phase, [10, 11, 30]. It rather passes the sole of the supporting foot, from the heel to the toe.

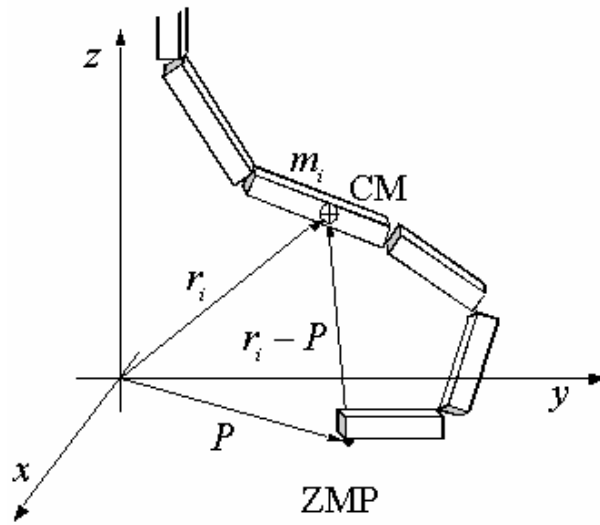


Figure 4.3. Kinematic Chain for Center of Mass.

A natural ZMP trajectory during the human walk cycle is illustrated in Fig. 4.4. We believe that using natural ZMP reference trajectories for gait generation will result in a more natural and energy efficient CoM trajectory. In fact, already reported results also show that -since the resulting CoM trajectory oscillations are smoother- using variable ZMP trajectories result in more energy efficient trajectories [30].

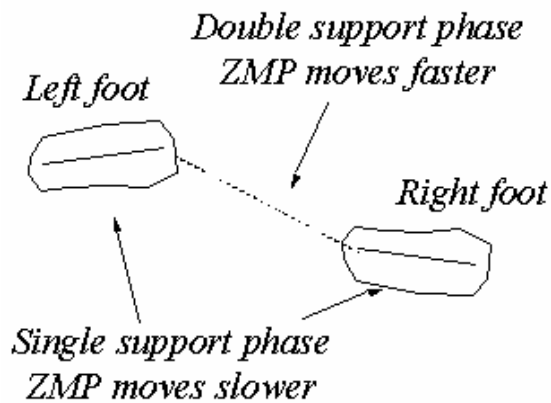


Figure 4.4. A Natural ZMP trajectory.

4.3. Exact Solution of Linear Inverted Pendulum Model for Fixed ZMP

In this Section the exact solution of the LIPM equations (with given fixed ZMP trajectories), which is done in [29], is shown. Recall the ZMP equations (4.5) and (4.6).

$$p_x = c_x - \frac{1}{\omega_n^2} \ddot{c}_x$$

$$p_y = c_y - \frac{1}{\omega_n^2} \ddot{c}_y$$

where $\omega_n^2 = \frac{g}{z_c}$.

In order to get an intuition about these equations

Rearranging these equations,

$$\ddot{c}_x = \omega_n^2 c_x - \omega_n^2 p_x \quad (4.8)$$

$$\ddot{c}_y = \omega_n^2 c_y - \omega_n^2 p_y \quad (4.9)$$

From the equations (4.8) and (4.9) applying Laplace transform,

$$C_x(s) = \frac{1}{1 - \frac{1}{\omega_n^2} s^2} \left[p_x(s) - \frac{1}{\omega_n^2} C_x(0)s - \frac{1}{\omega_n^2} \dot{C}_x(0) \right] \quad (4.10)$$

$$C_y(s) = \frac{1}{1 - \frac{1}{\omega_n^2} s^2} \left[p_y(s) - \frac{1}{\omega_n^2} C_y(0)s - \frac{1}{\omega_n^2} \dot{C}_y(0) \right] \quad (4.11)$$

In (4.10) and (4.11) the following fixed ZMP trajectories are going to be used for the exact solution calculation. In Fig. 4.5. the x -axis (for saggital plane) reference for ZMP trajectory, in Fig. 4.6, the y -axis (for frontal plane) reference for ZMP trajectory, and in Fig. 4.7, the resulting ZMP trajectory in the $x - y$ plane can be seen. Note that Fig. 4.6 also indicates the foot placement positions in the $x - y$ plane.

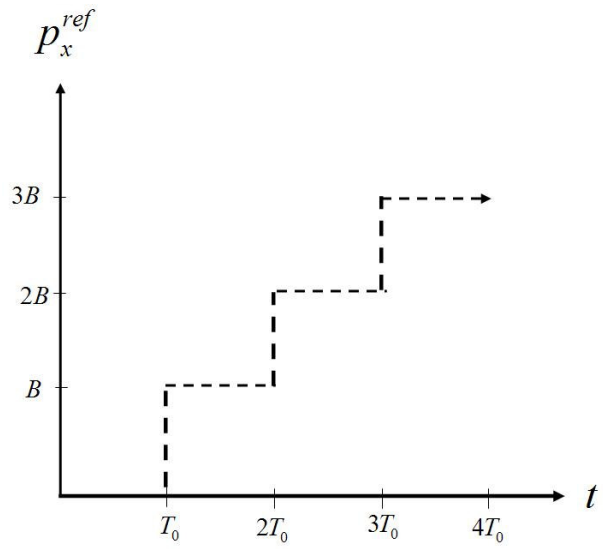


Figure 4.5. p_x^{ref} , x-axis ZMP reference trajectory

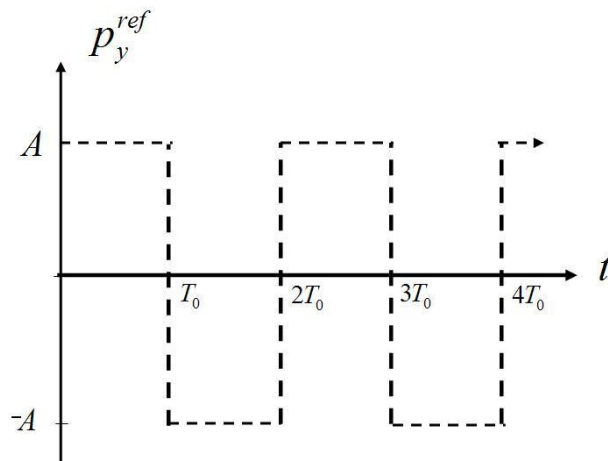


Figure 4.6. p_y^{ref} , y-axis ZMP reference trajectory

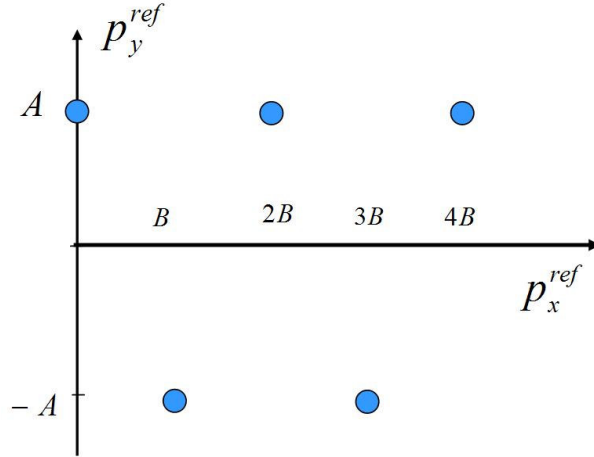


Figure 4.7 $p_y^{ref} - p_x^{ref}$ on $x - y$ plane ZMP reference trajectory / Step Positions

The ZMP reference trajectories in Fig. 4.4 and Fig. 4.5 can be expressed as follows.

$$p_x^{ref} = B \sum_{k=1}^{\infty} 1(t - kT_0) \quad (4.12)$$

$$p_y^{ref} = A1(t) + 2A \sum_{k=1}^{\infty} (-1)^k 1(t - kT_0) \quad (4.13)$$

Taking the Laplace transform of (4.12) and (4.13) and substituting it to (4.10) and (4.11) with zero initial conditions the following equations can be derived.

$$C_x(s) = \frac{1}{1 - \frac{1}{\omega_n^2} s^2} \left[\frac{B}{s} e^{-T_0 s} + \frac{B}{s} e^{-2T_0 s} + \frac{B}{s} e^{-3T_0 s} + \dots \right] \quad (4.14)$$

$$C_y(s) = \frac{1}{1 - \frac{1}{\omega_n^2} s^2} \left[\frac{A}{s} - \frac{2A}{s} e^{-T_0 s} + \frac{2A}{s} e^{-2T_0 s} - \frac{2A}{s} e^{-3T_0 s} + \dots \right] \quad (4.15)$$

Since;

$$\frac{1}{1 - \frac{1}{\omega_n^2} s^2} \frac{1}{s} = \frac{1}{s} - \frac{s}{(s^2 - \omega_n^2)}$$

(4.14) and (4.15) can be rearranged to derive the following transfer functions.

$$C_x(s) = B\left(\frac{1}{s} - \frac{s}{s^2 - \omega_n^2}\right)e^{-T_0s} + B\left(\frac{1}{s} - \frac{s}{s^2 - \omega_n^2}\right)e^{-2T_0s} + B\left(\frac{1}{s} - \frac{s}{s^2 - \omega_n^2}\right)e^{-3T_0s} + \dots \quad (4.16)$$

$$C_y(s) = A\left(\frac{1}{s} - \frac{s}{s^2 - \omega_n^2}\right) - 2A\left(\frac{1}{s} - \frac{s}{s^2 - \omega_n^2}\right)e^{-T_0s} + 2A\left(\frac{1}{s} - \frac{s}{s^2 - \omega_n^2}\right)e^{-2T_0s} - \dots \quad (4.17)$$

Finally, the exact reference trajectories of the CoM can be obtained by applying inverse Laplace transformations to (4.16) and (4.17) as follows.

$$C_x(s) = B(1 - \cosh \omega_n(t - T_0))l(t - T_0) + B(1 - \cosh \omega_n(t - 2T_0))l(t - 2T_0) + \dots \quad (4.18)$$

$$= B \sum_{k=1}^{\infty} (1 - \cosh \omega_n(t - kT_0))l(t - kT_0)$$

$$C_y(s) = A(1 - \cosh \omega_n(t - T_0)) - 2A(1 - \cosh \omega_n(t - T_0))l(t - T_0) + \dots \quad (4.19)$$

$$= 2A \sum_{k=1}^{\infty} (-1)^k (1 - \cosh \omega_n(t - kT_0))l(t - kT_0)$$

Although (4.18) and (4.19) are the exact solutions for the ordinary differential equations (4.5) and (4.6), in practice they are difficult to be used robustly for a real biped walking robot since they are composed of numerically unbounded $\cosh(\cdot)$ functions. Furthermore, they are unstable and very sensitive to the variation of ω_n . Therefore, an approximated solution composed of bounded $\sin(\cdot)$ functions is suggested to serve as a robust CoM trajectory in the following section.

4.4. Planning an Approximate Solution

In this section the approximate solution for LIPM equations done in [29] is shown. First an odd function with period T_0 is introduced from the x -directional reference ZMP p_x^{ref} of (4.12) as follows.

$$\begin{aligned} p'_x(t) &:= p_x^{ref}(t) - \frac{B}{T_0} \left(t - \frac{T_0}{2} \right) \\ &= \frac{B}{T_0} \left(t - \frac{T_0}{2} \right) \quad \text{and} \quad p'_x(t+T_0) = p'_x(t) \end{aligned} \quad (4.20)$$

Then assuming that the x -directional reference trajectory of CoM has the following form by using Fourier series,

$$C_x^{ref}(t) = \frac{B}{T_0} \left(t - \frac{T_0}{2} \right) + \sum_{n=1}^{\infty} \left[a_n \cos\left(\frac{n\pi}{T_0} t \right) + b_n \sin\left(\frac{n\pi}{T_0} t \right) \right] \quad (4.21)$$

Then applying (4.21) to the ZMP differential equation (4.5) the following relation can be found.

$$p_x^{ref}(t) = \frac{B}{T_0} \left(t - \frac{T_0}{2} \right) + p'_x(t) \quad (4.22)$$

where

$$p'_x(t) = \sum_{n=1}^{\infty} \left[a_n \left(1 + \frac{n^2 \pi^2}{T_0^2 \omega_n^2} \right) \cos\left(\frac{n\pi}{T_0} t \right) + b_n \left(1 + \frac{n^2 \pi^2}{T_0^2 \omega_n^2} \right) \sin\left(\frac{n\pi}{T_0} t \right) \right] \quad (4.23)$$

Here in (4.22) the form of the odd function $p'_x(t)$ can be seen in Fig. 4.8. Since $p'_x(t)$ is an odd function with period T_0 , the coefficients $a_n = 0$ and b_n can be found by solving the following equation.

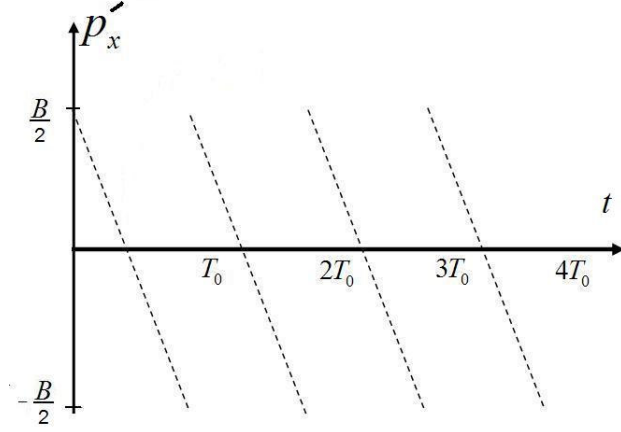


Figure 4.8. $p'_x(t)$ Introduced odd Function.

$$b_n \left(1 + \frac{n^2 \pi^2}{T_0^2 \omega_n^2} \right) = \frac{2}{T_0} \int_0^{T_0} p'_x(t) \sin \left(\frac{n\pi}{T_0} t \right) dt \quad (4.24)$$

Finally, b_n can be found as follows.

$$b_n = \frac{BT_0^2 \omega_n^2 (1 + \cos n\pi)}{n\pi (T_0^2 \omega_n^2 + n^2 \pi^2)} \quad (4.25)$$

As a result, the x -directional reference trajectory of CoM can be found by substituting (4.25) to (4.21) as follows.

$$C_x^{ref}(t) = \frac{B}{T_0} \left(t - \frac{T_0}{2} \right) + \sum_{n=1}^{\infty} \left[\frac{BT_0^2 \omega_n^2 (1 + \cos n\pi)}{n\pi (T_0^2 \omega_n^2 + n^2 \pi^2)} \sin \left(\frac{n\pi}{T_0} t \right) \right] \quad (4.26)$$

On the other hand, since the y -directional reference ZMP $p'_y(t)$ of (4.13) is an odd function with period T_0 the y -directional reference can be found in a similar manner as follows.

$$C_y^{ref}(t) = \sum_{n=1}^{\infty} \left[\frac{2AT_0^2 \omega_n^2 (1 - \cos n\pi)}{n\pi (T_0^2 \omega_n^2 + n^2 \pi^2)} \sin \left(\frac{n\pi}{T_0} t \right) \right] \quad (4.27)$$

The resulting CoM trajectories for x and y axes can be seen in Fig. 4.9 and from Fig. 4.10.

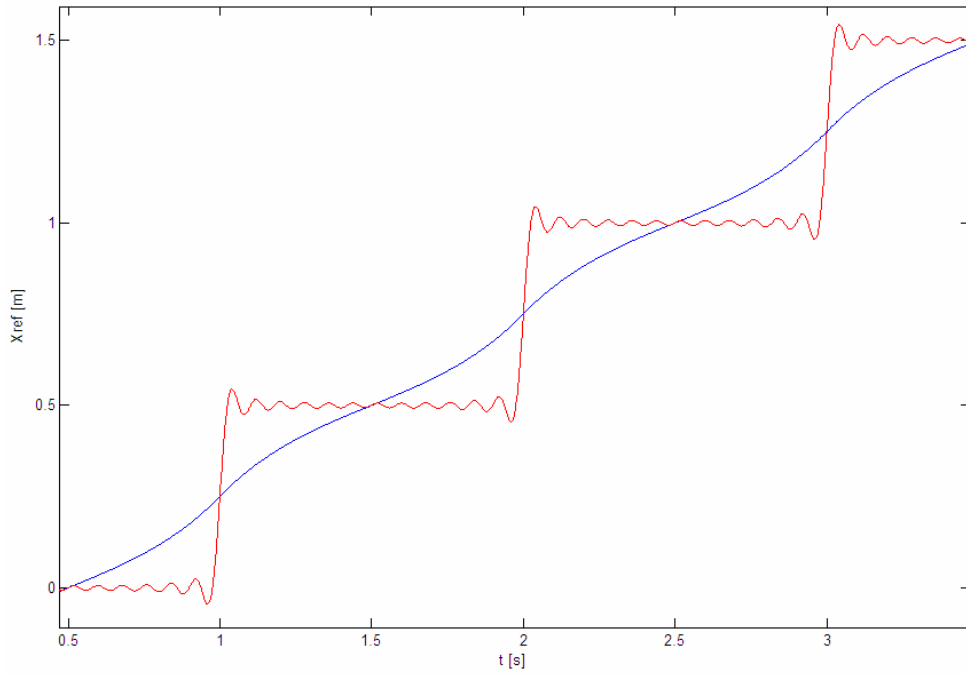


Figure 4.9. C_x Reference trajectory for x -axis (Sagittal Plane, $B=0.5$, $T_0=1$).

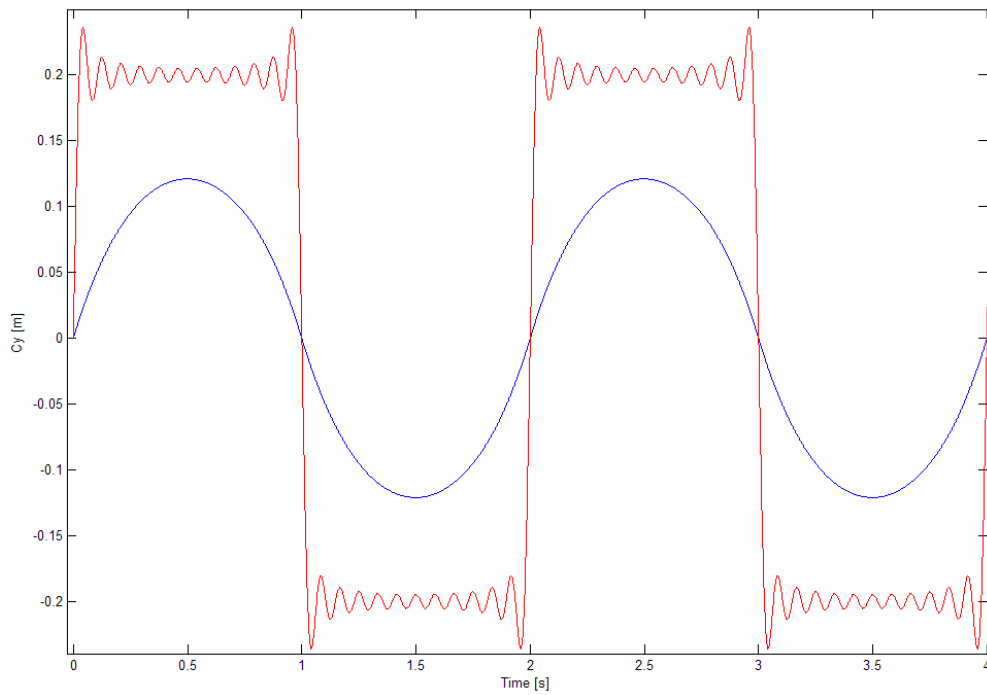


Figure 4.10. C_y Reference Trajectory for y -axis (Frontal Plane, $A=0.5$).

In Fig. 4.9 it can be observed that the CoM is passing through acceleration and deceleration phases in such a way that the given ZMP reference is achieved. Similarly in Fig. 4.10 the CoM is forming a *sine*-like curve to satisfy the ZMP reference.

4.5. Introduction of Natural ZMP Reference Trajectories by Fourier Approximation to Obtain CoM Trajectories

As discussed in the previous sections the ZMP trajectory in a human walking cycle is not fixed at a point at certain periods but it travels under the supporting polygon. In the single support phase the ZMP travels from heel to the toe of the foot and in the double support phase it travels from the toe of the supporting foot to the heel of the swinging foot [10, 11]. In this context the x -directional reference ZMP trajectory p_x^{ref} (Fig. 4.11) is introduced, which is an improvement to Choi, Y. et. al's work in [29].

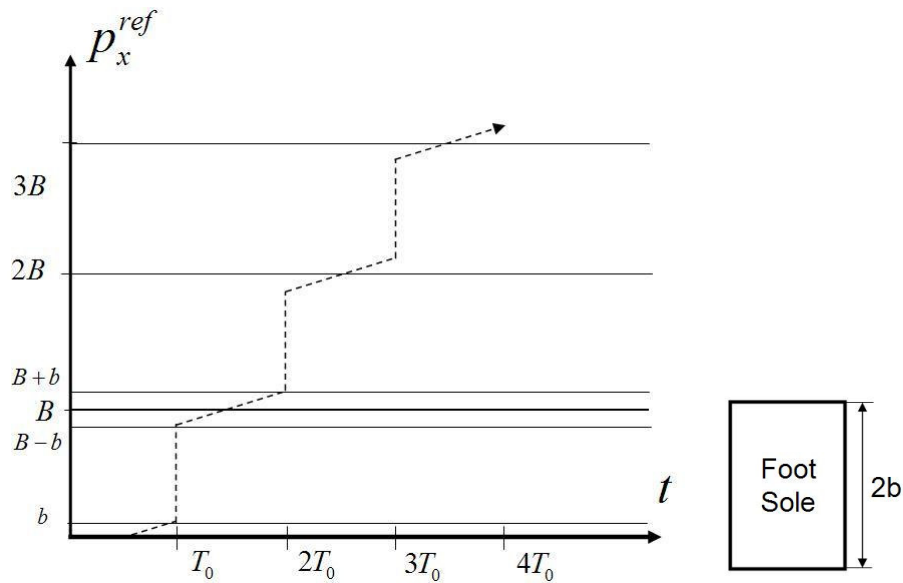


Figure 4.11. Natural ZMP reference trajectory.

Here b is the half length of the foot sole. It can be observed that in this trajectory ZMP travels starts from zero and advances in time under the sole of the foot in the initial single support phase and from heel to the toe of the foot in the further single support phases. By the same procedure followed in the previous sections the following odd function p'_x with period T_0 from the x -directional reference ZMP p_x^{ref} is introduced, Fig.4.12.

$$\begin{aligned}
p'_x(t) &:= p_x^{ref}(t) - \frac{B}{T_0} \left(t - \frac{T_0}{2} \right) \\
&= \frac{B}{T_0} \left(t - \frac{T_0}{2} \right) \quad \text{and} \quad p'_x(t+T_0) = p'_x(t)
\end{aligned} \tag{4.28}$$

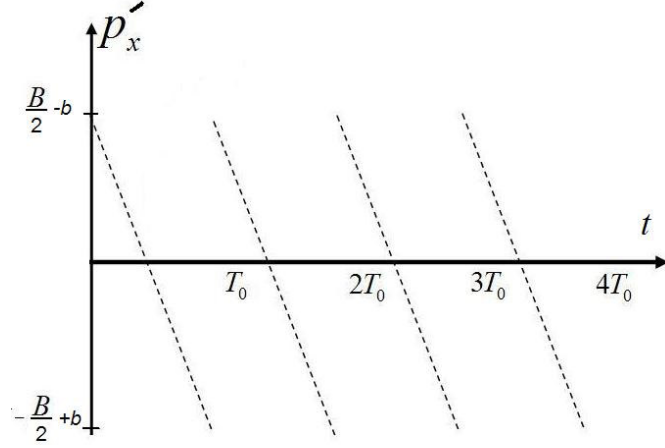


Figure 4.12. $p'_x(t)$ New introduced odd function.

Applying the same procedure from (4.20) to (4.25) the new b_n coefficient can be found as follows.

$$b_n = \frac{(B - 2b)T_0^2 \omega_n^2 (1 + \cos n\pi)}{n\pi(T_0^2 \omega_n^2 + n^2 \pi^2)} \tag{4.29}$$

Hence the natural CoM trajectory is found as follows.

$$C_x^{ref}(t) = \frac{B}{T_0} \left(t - \frac{T_0}{2} \right) + \sum_{n=1}^{\infty} \left[\frac{(B - 2b)T_0^2 \omega_n^2 (1 + \cos n\pi)}{n\pi(T_0^2 \omega_n^2 + n^2 \pi^2)} \sin \left(\frac{n\pi}{T_0} t \right) \right] \tag{4.30}$$

The resulting C_x trajectory can be seen in Fig. 4.13. Note that the resulting C_x trajectory is smoother (showed in dashed line) than the conventional C_x trajectory with fixed ZMP, which was introduced by Choi, Y. et. al [29]. The smoothness of the resulting trajectory implies that the acceleration differences are less when compared with the conventional C_x trajectory with fixed ZMP. This also implies that less energy is necessary to track the C_x trajectory with variable ZMP.

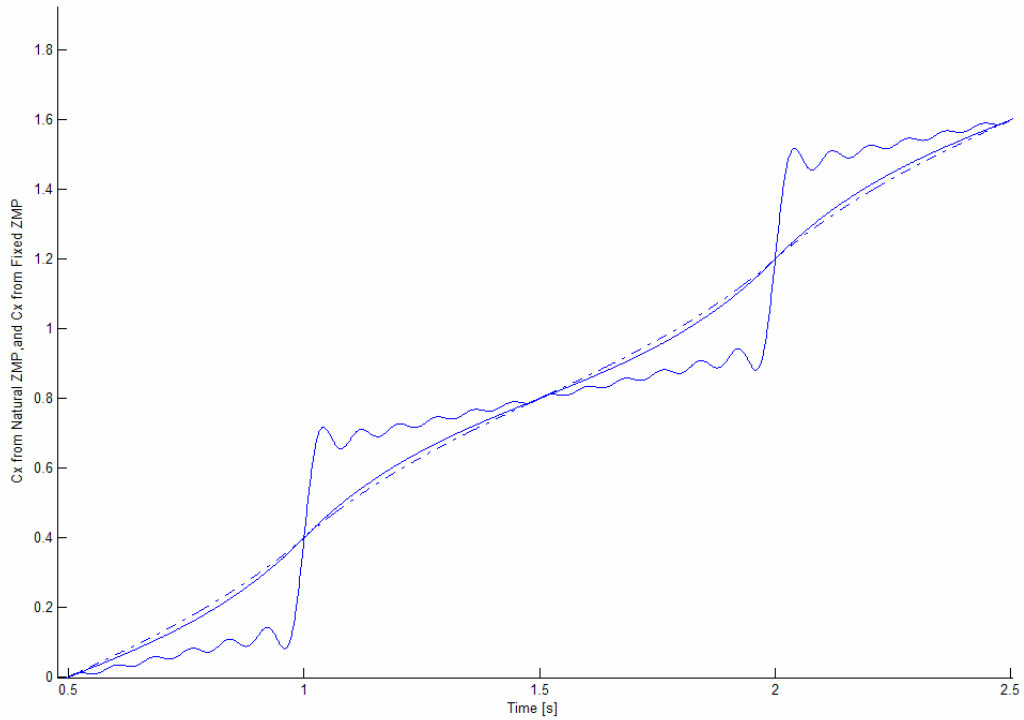


Figure 4.13. C_x Trajectory w/ variable ZMP (Solid line) and w fixed ZMP (dashed line)

4.6. Introducing Double Support Phase to ZMP Reference Trajectories.

In this section the introduction of double support phases to previously used reference ZMP trajectories will be addressed which is also an improved version to method at [29]. Adding double support phase to reference ZMP trajectories in both x and y axes by the previously used method in Section 4.3, which is to blend lines with different slopes, makes it impossible to overcome such a problem. Instead to overcome this problem the so-called Lanczos Sigma Factor is used for such a task.

The non-uniform convergence of the Fourier series for discontinuous functions is known as Gibbs Phenomenon in the literature. There are complex methods to smooth the Gibbs Phenomenon. One method is the so-called Lanczos Sigma Factor. In this approximation a function is multiplied by the coefficients in the Fourier partial sums. This function is a complex *sine* function involving the period of the original function.

Fourier series by the Lanczos Sigma Factor can be rewritten as follows.

$$f(\theta) = \frac{a_0}{2} + \sum_{n=1}^{m-1} \sin c\left(\frac{n\pi}{m}\right) [a_n \cos(n\theta) + b_n \sin(n\theta)] \quad (4.31)$$

The resulting effect of the Lanczos Sigma Factor can be seen in Fig. 4.14 and Fig. 4.15.

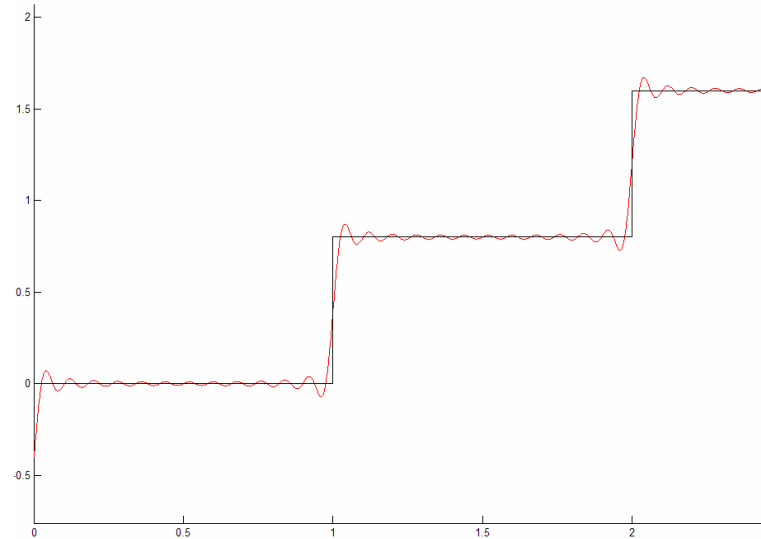


Figure 4.14. Fourier approximation w/o Lanczos sigma factor.

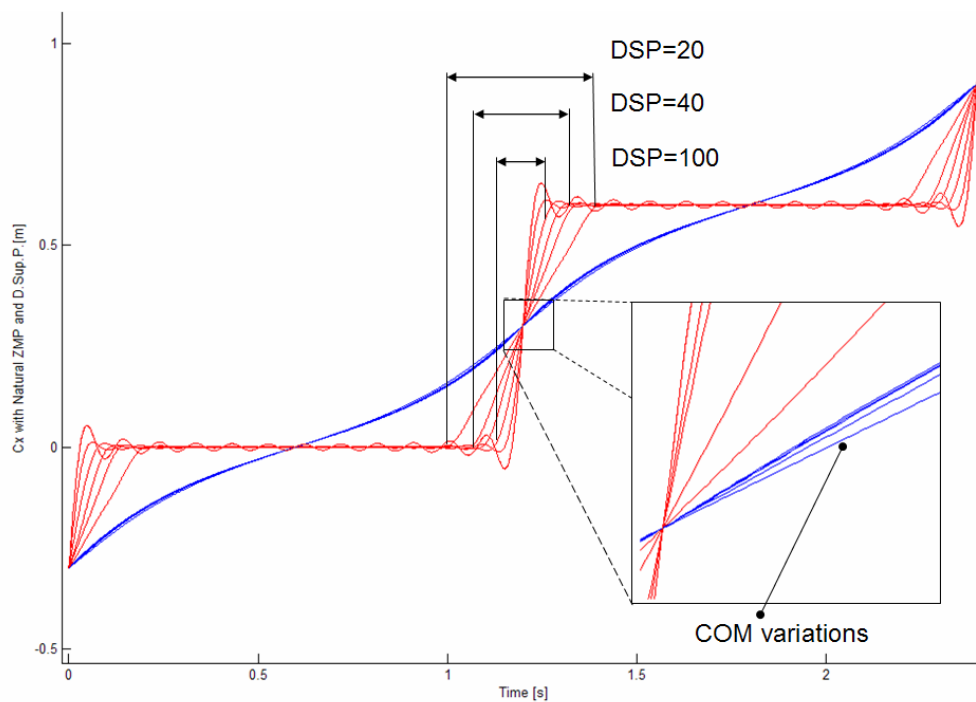


Figure 4.15. Fourier approximation w/ Lanczos sigma factor.

In this example the Double Support Parameter DSP of the Lanczos Sigma Factor ($\sin c(\frac{n\pi}{DSP})$) is used to attain double support phases in the reference ZMP trajectory.

Notice that in Fig. 4.15 the duration of the double support phase is tuned by setting appropriate values to the DSP parameter. Also observe the variations of the CoM trajectory corresponding to different double support phase durations.

Further the found Natural CoM trajectories for $x - y$ axes are as follows.

$$C_x^{ref}(t) = \frac{B}{T_0} \left(t - \frac{T_0}{2} \right) + \sum_{n=1}^{\infty} \left[(B - 2b) \frac{BT_0^2 \omega_n^2 (1 + \cos n\pi)}{n\pi (T_0^2 \omega_n^2 + n^2 \pi^2)} \sin c\left(\frac{n\pi}{DSP}\right) \sin\left(\frac{n\pi}{T_0} t\right) \right] \quad (4.32)$$

$$C_y^{ref}(t) = \sum_{n=1}^{\infty} \left[\frac{2AT_0^2 \omega_n^2 (1 - \cos n\pi)}{n\pi (T_0^2 \omega_n^2 + n^2 \pi^2)} \sin c\left(\frac{n\pi}{DSP}\right) \sin\left(\frac{n\pi}{T_0} t\right) \right] \quad (4.33)$$

In addition the Natural ZMP trajectories for $x - y$ axes are as follows.

$$p_{xNatural}^{ref}(t) = \frac{B}{T_0} \left(t - \frac{T_0}{2} \right) + \sum_{n=1}^{\infty} \left[\frac{(B - 2b)(1 + \cos n\pi)}{n\pi} \sin c\left(\frac{n\pi}{DSP}\right) \sin\left(\frac{n\pi}{T_0} t\right) \right] \quad (4.34)$$

$$p_{yNatural}^{ref}(t) = \sum_{n=1}^{\infty} \left[\frac{2A(1 - \cos n\pi)}{n\pi} \sin c\left(\frac{n\pi}{DSP}\right) \sin\left(\frac{n\pi}{T_0} t\right) \right] \quad (4.35)$$

In Fig. 4.16 and Fig. 4.17 it can be observed that the new C_x^{ref} is smoother than both of the previous versions. This, in fact, is an outcome of the novel approach of embedding both the varying ZMP reference and the double support phases in to Fourier approximation to LIPM equations. Also it can be observed that the Gibbs Phenomenon effect is almost disappeared and a smoother ZMP reference approximation is achieved. Moreover, by varying the parameters different types of gaits can be generated.

As an example, trajectory for the walking parameters close to a human's is given in Fig. 4.16, and in Fig. 4.17 ($A=.15[m]$, $B=.6[m]$, $b=[.14]$ and $T_0 =1 [s]$).

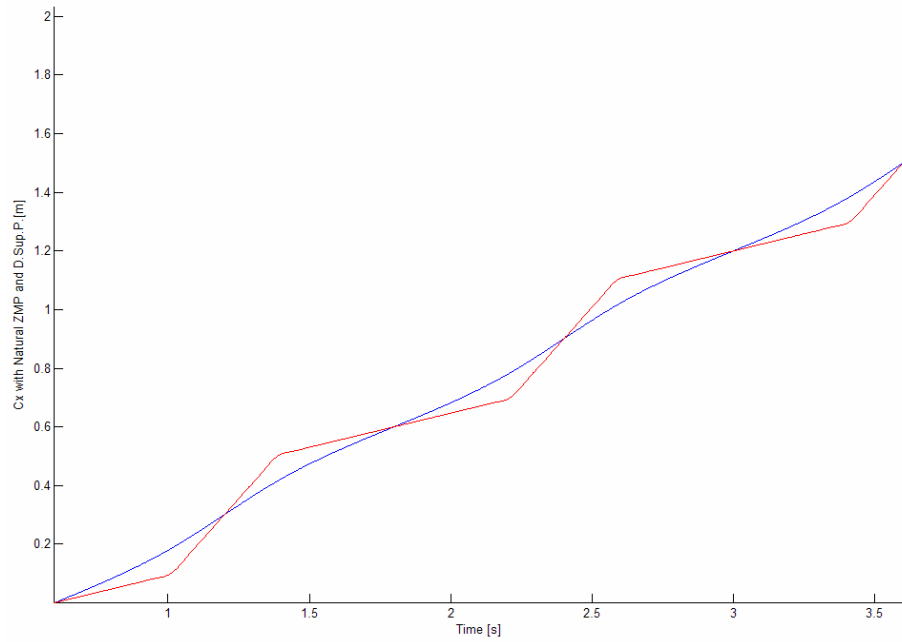


Figure 4.16. Natural C_x reference with parameters close to human walk.

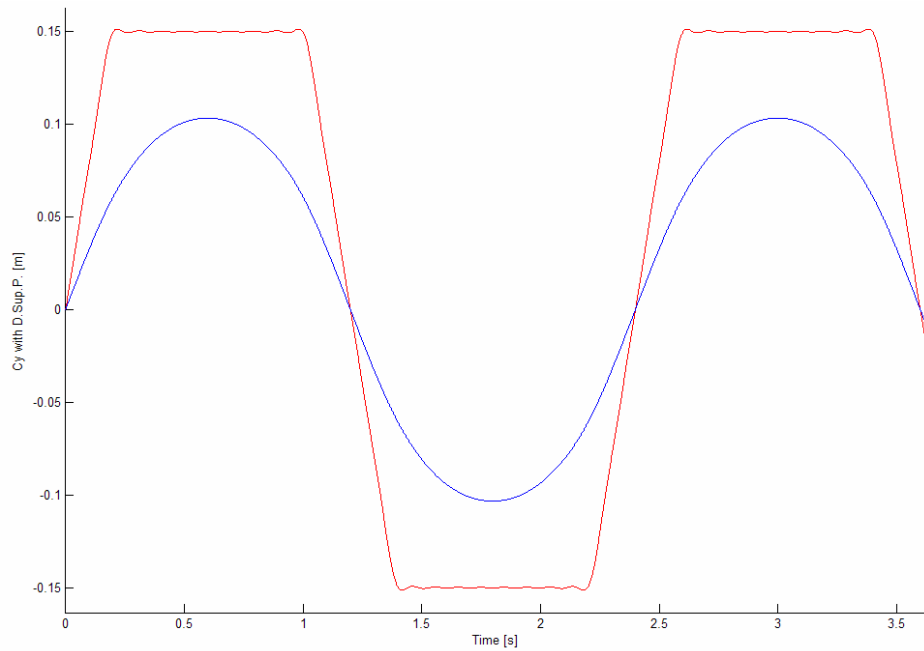


Figure 4.17. Natural C_y reference with parameters close to human walk.

Chapter 5

5. COORDINATION and CONTROL of LOCOMOTION

The discussion previous chapter develops how a CoM reference can be obtained from a given ZMP reference trajectory. This chapter firstly discusses how swing foot position references are obtained from the Fourier series approximation of the ZMP reference trajectory and the generated CoM reference trajectory. Secondly, the control algorithm, which consists of five lower level position and force controller building blocks, is explained.

As shown in Fig. 5.1, the swing foot position references are obtained from the ZMP and the CoM reference curves. Fig. 5.2 shows the directions of the world frame. The origin of the world frame is at the ground level. The reference trajectories are described in the fixed world coordinate frame. The robot trunk (or body) coordinate frame is initially positioned just over the world coordinate frame.

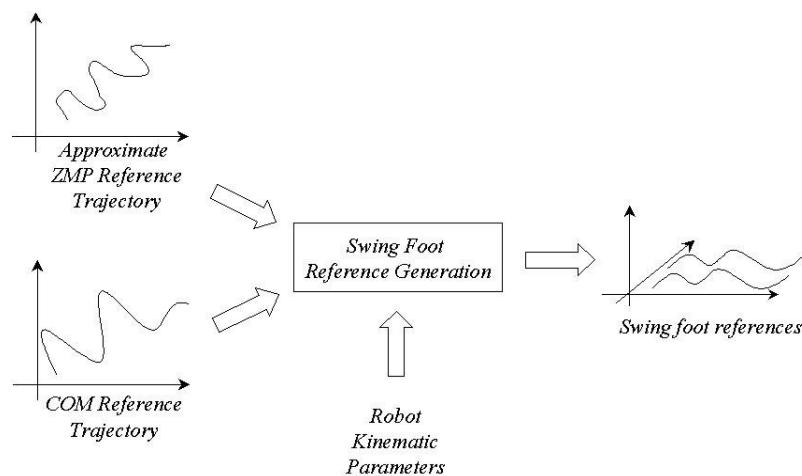


Figure 5.1. The swing foot position references are obtained from ZMP and CoM references.

For simplicity, the generated CoM position reference is used as a reference for the center of mass of the trunk (which is not necessarily at the trunk coordinate frame origin). It is assumed that the position of the center of mass of the trunk is known as expressed in the trunk coordinate frame.

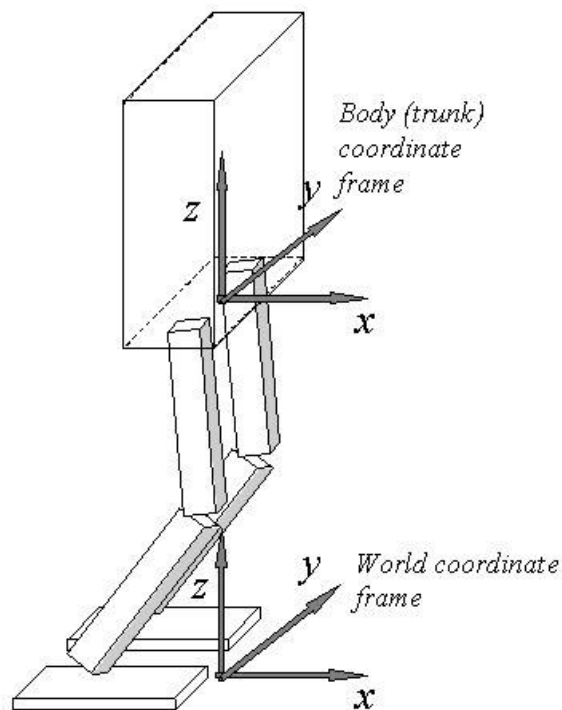
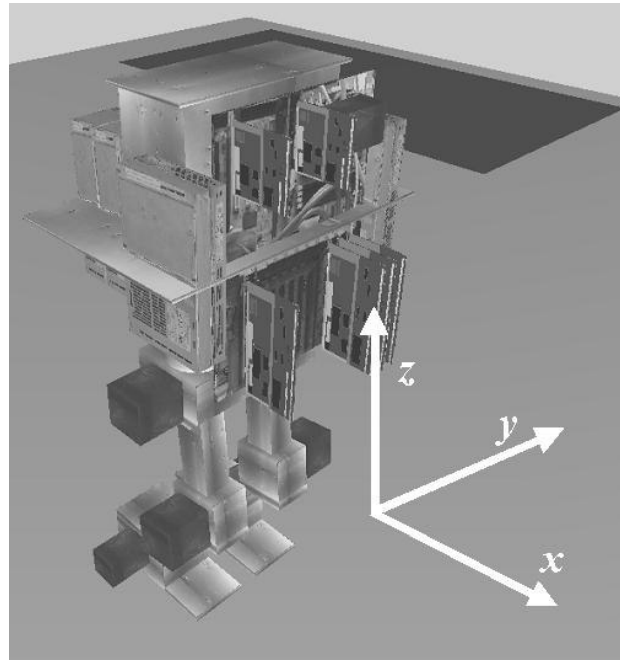


Figure 5.2. World frame directions.

Fig. 5.3 shows the y -component of a typical ZMP curve after Fourier series approximation together with the generated CoM reference in this direction. It should be noted that the ZMP position reference is not defined before the end of a certain initialization phase shown in Fig. 5.4. In this phase the robot trunk CoM follows an initialization trajectory in the y -direction. The initialization reference trajectory followed is a smooth one avoiding unnecessary oscillations before the periodic stepping motion begins. The curve is in the form of a shifted cosine function over an half period, climbing from zero to the amplitude of the CoM reference y -component. The configurations of the robot before and after the initialization phase are shown in Fig. 5.5.

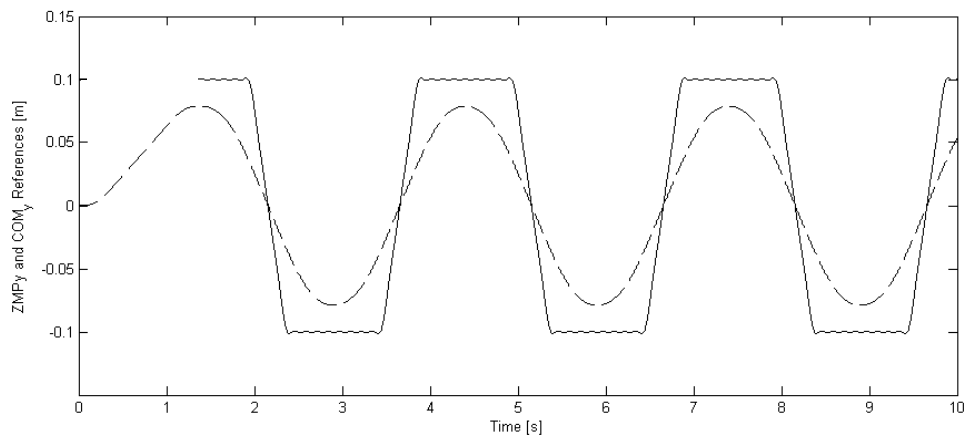


Figure 5.3. The ZMP and CoM (dashed) position reference y -components.

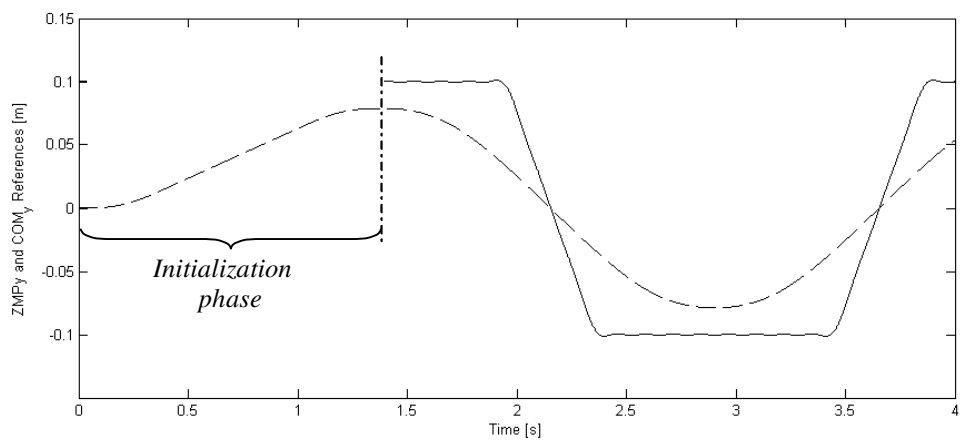


Figure 5.4. The CoM reference y -component (dashed) in the initialization phase.

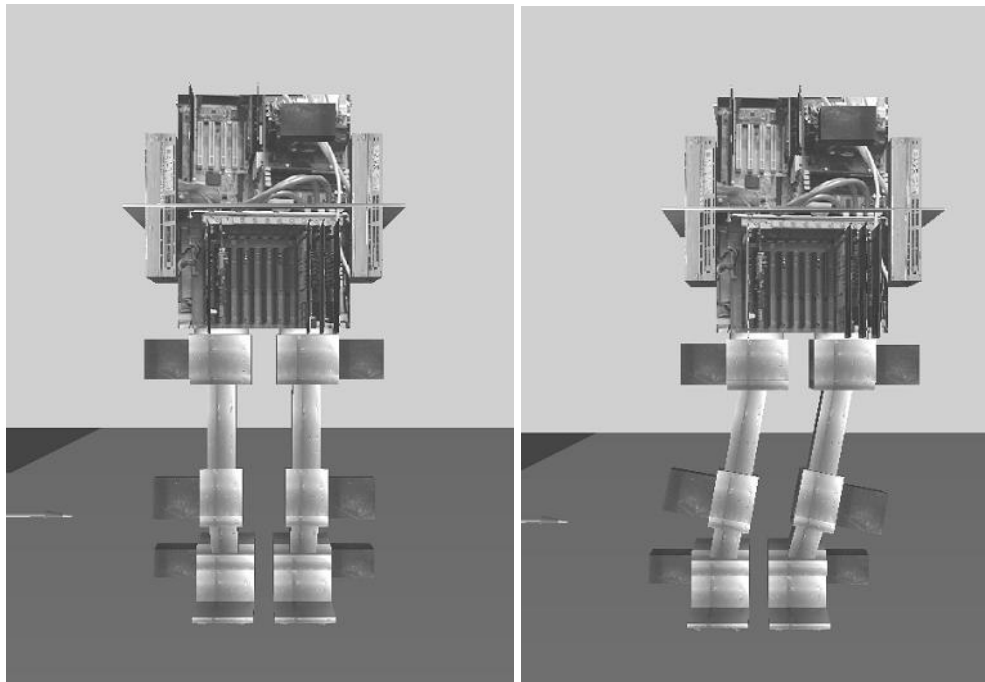


Figure 5.5. Robot configurations at the beginning (left) and at the end (right) of the configuration phase.

The flat regions of the of the typical ZMP curve y-component indicate the single support phases. The corners of this curve can easily be detected in software implementation. In Fig. 5.6 the beginning of right and left support phases are indicated by “o” and “+” signs respectively. When one of the feet is in the single support phase the other one is in the swing phase and therefore the timing information for the support phases contains the timing information for the swing phases too. The duration of the swing is measured as the width of the flat regions.

The height of the step is a design variable in the order of few centimeters for a human sized biped. The up and down motion of the swing foot is planned as a shifted cosine curve with an amplitude equal to the half of the step height and period equal to the swing duration. Typical swing reference positions of the right and left legs in the z direction are shown in Fig. 5.7, together with the y-component of the ZMP position reference.

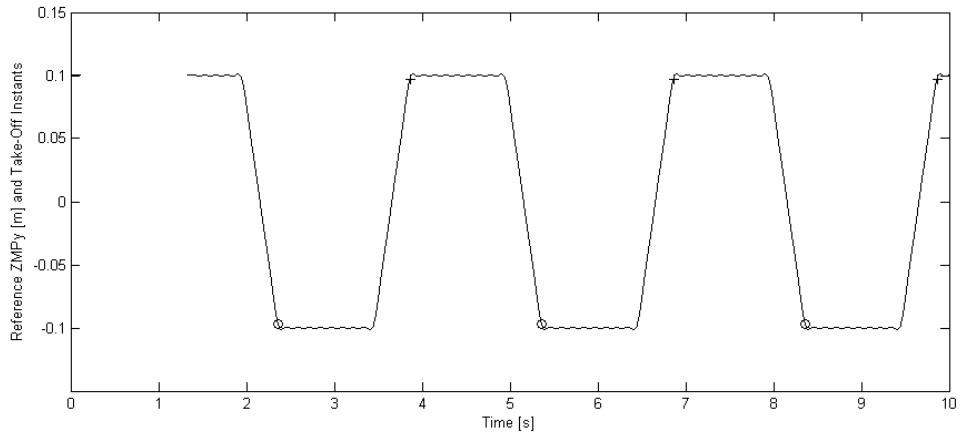


Figure 5.6. Typical ZMP reference position in the y-direction and swing timing detection.

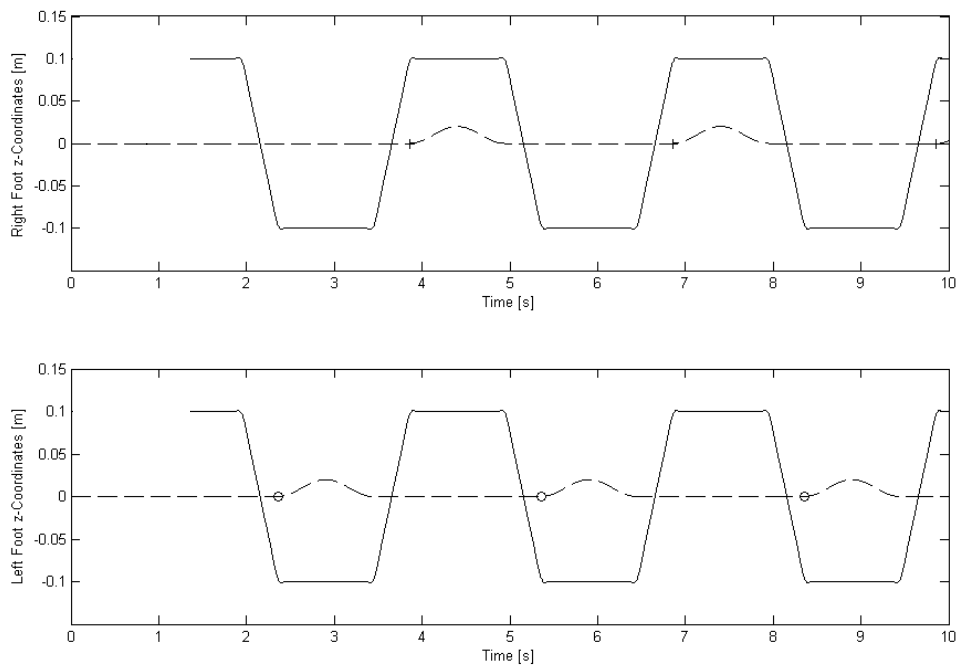


Figure 5.7. Typical swing foot z-direction position references (dashed) and their timing with respect to the ZMP references (solid curve).

The x -components of the ZMP and CoM references are displayed in figures 5.8 and 5.9. The locomotion is achieved by applying z -direction references to the swing feet in their respective swing periods. The x -direction foot position references are shown in figures 5.10 and 5.11. These references are constant in the support periods, and they rise smoothly to keep up with the CoM position reference in the swing periods. The smooth step increment is realized again in the form of a shifted cosine function. The amplitude of the cosine function is half of the step size, which is a design parameter. The period of the cosine function is twice the swing period, and the function is applied over its half period as the x -reference. The offset between the initial CoM x -position and the foot positions is due to the fact that the foot coordinate frame centers are behind the CoM for a stable static configuration of the robot.

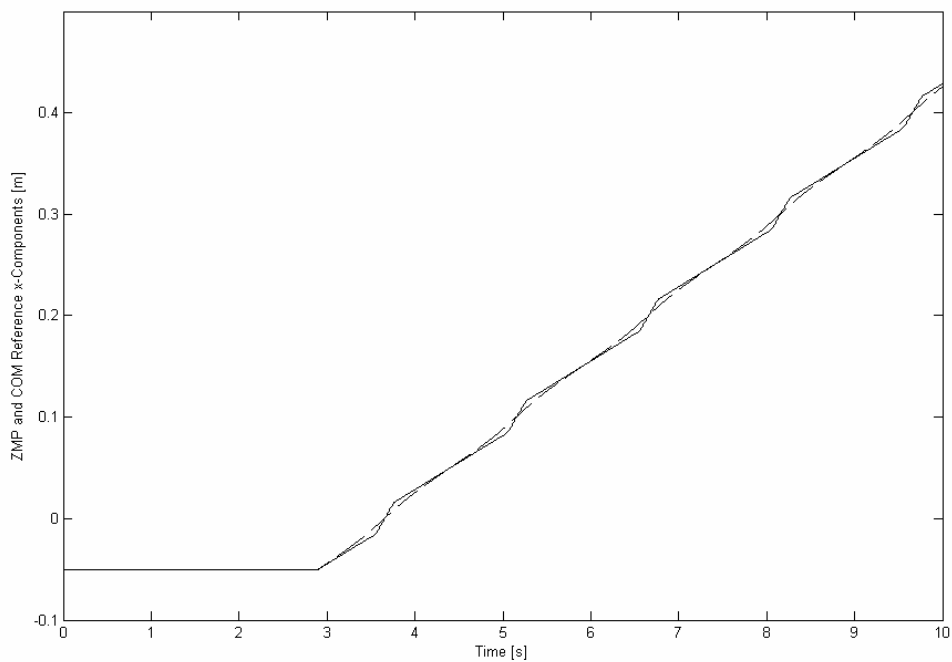


Figure 5.8. The ZMP (solid) and CoM (dashed) reference x -components.

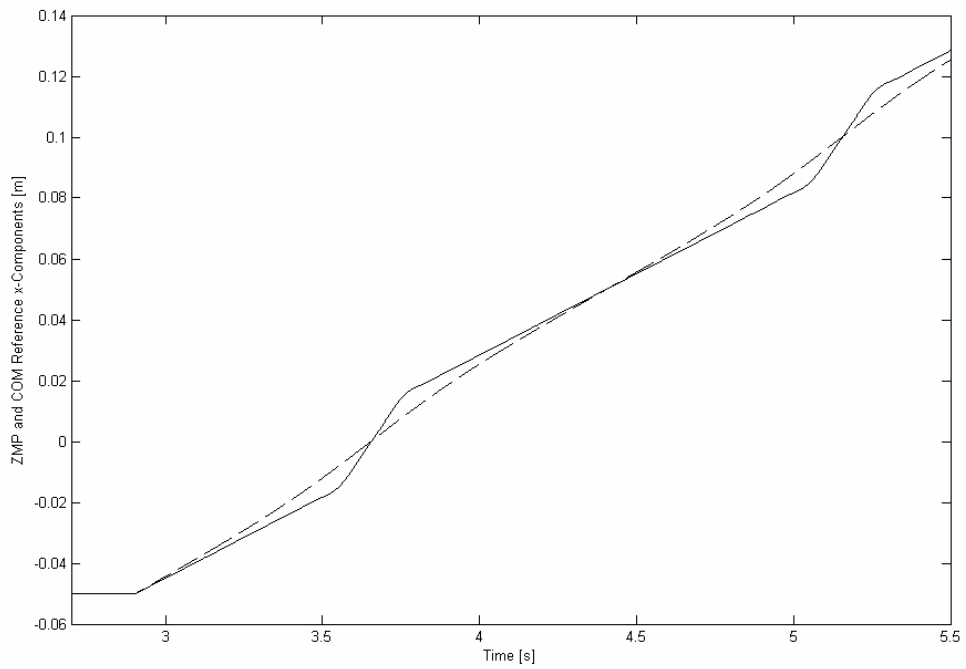


Figure 5.9. The ZMP (solid) and CoM (dashed) reference x -components, a closer view.

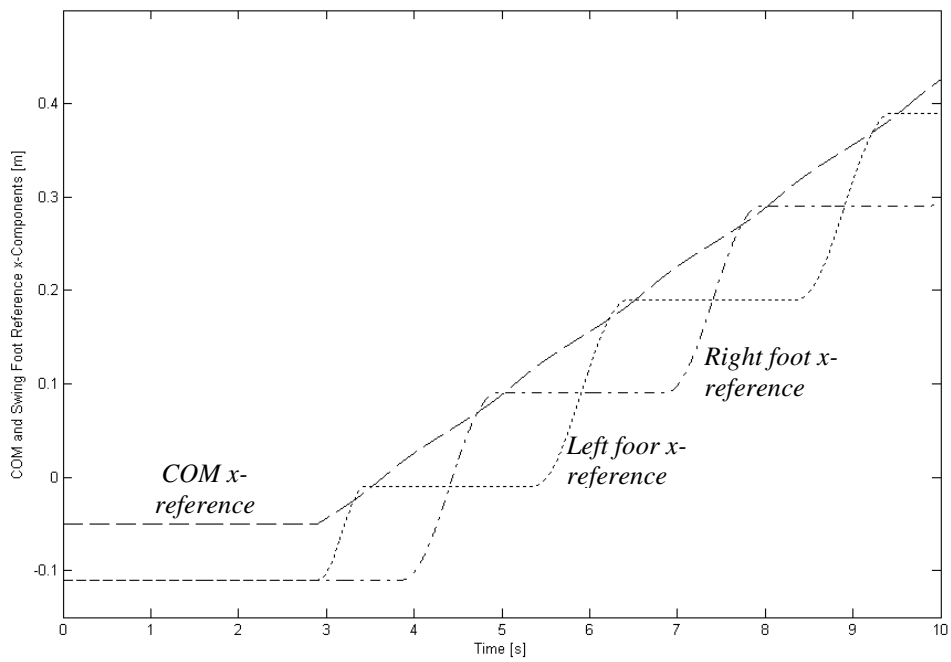


Figure 5.10. CoM reference and swing foot x -components.

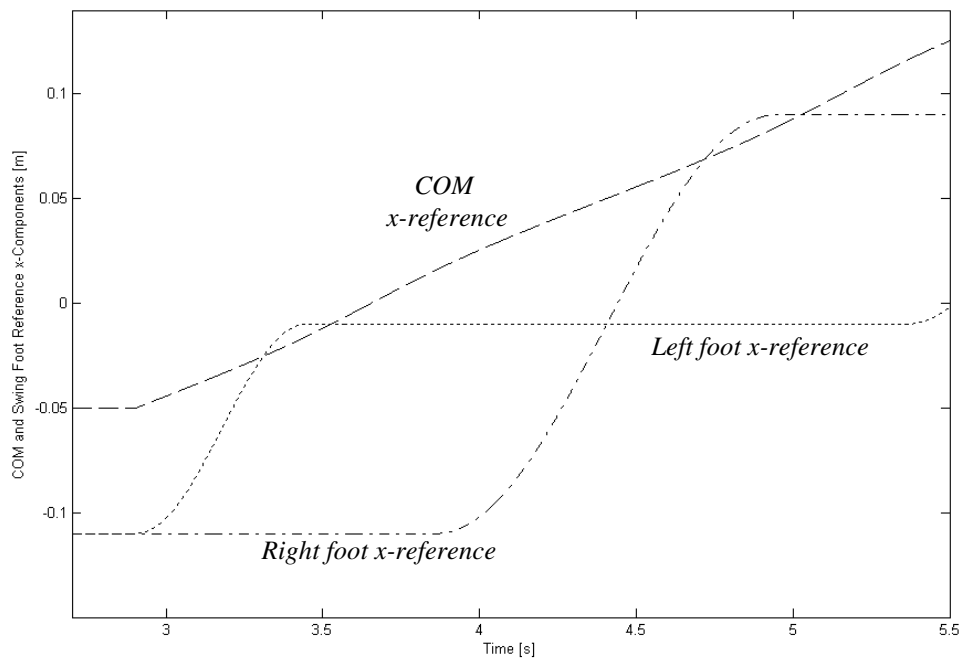


Figure 5.11. CoM reference and swing foot x-components, a closer view.

As mentioned above, the control algorithm consists of five lower level position and force controller building blocks (Fig. 5.12). Swing foot references, or alternatively, the swing timing is determines the timing for switching between control structures. However, swing reference timing is not the only criterion to switch from one control mode to the other. Switching from swing to support controller before actually reaching the ground level and establishing stable contact with the ground can cause a sudden loss of the robot balance. Therefore, ground interaction force information is used and controller mode switching is not allowed before the z-direction component of the contact force exceeds a certain threshold value. The force threshold value is a design parameter. The support to swing switching times obey the swing timing without additional feedback from ground interaction forces. The CoM and swing foot references are employed in different modes of the control as shown in Fig. 5.13.

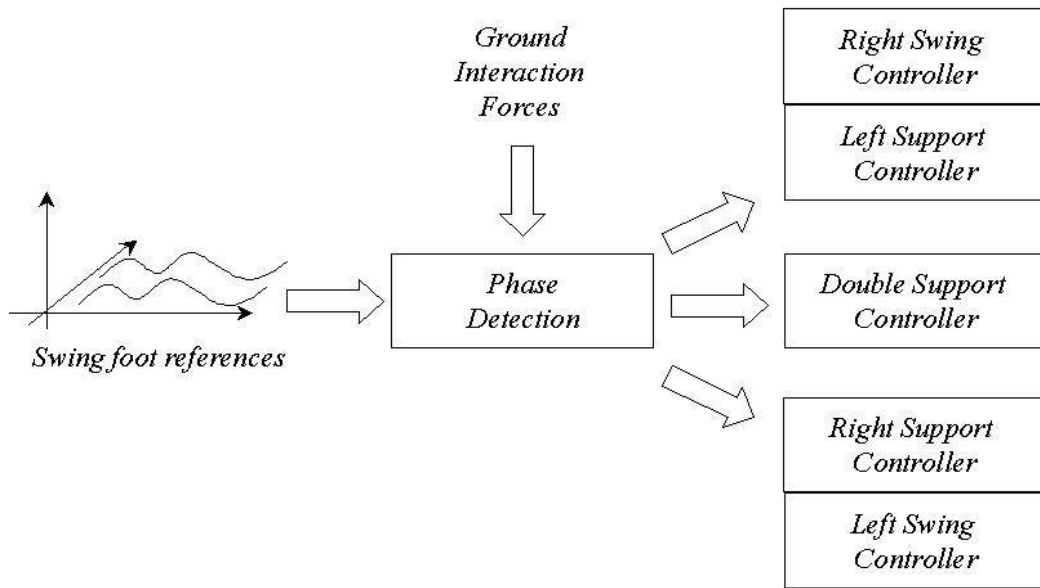


Figure 5.12. The switching between control modes is realized by processing the ground interaction force and swing foot reference timing.

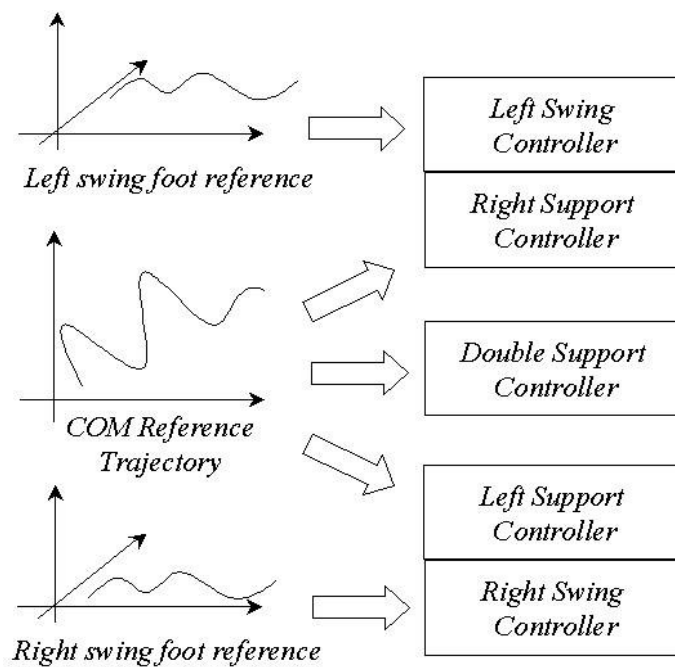


Figure 5.13. The position references used in different control modes.

The double support controller regards the biped robot as a trunk manipulated by two six-DOF arms with their bases positioned on the ground level (Fig. 5.14). The CoM position reference discussed above and fixed orientation reference with respect to the world coordinate frame are applied in a position control schemes for both manipulators. The position controllers running for the two manipulators (legs) are identical. Cartesian position and orientation errors are computed from the reference and actual position and orientations. These errors are reflected to the joint space errors by the use of inverse Jacobian relations. Independent joint controllers are employed for the joint space position control. The controllers for the two legs work almost independently. However, the Cartesian errors are scaled with different gains for the two legs before corresponding joint errors are computed (Fig. 5.15). The scaling factor for the right leg is proportional to the horizontal distance of the left foot coordinate center from the CoM and similarly, the scaling factor for the left leg is proportional to the horizontal distance of the right foot from the CoM. This rule is obtained experimentally and it performed well for the coordination of the two legs in the double support phase.

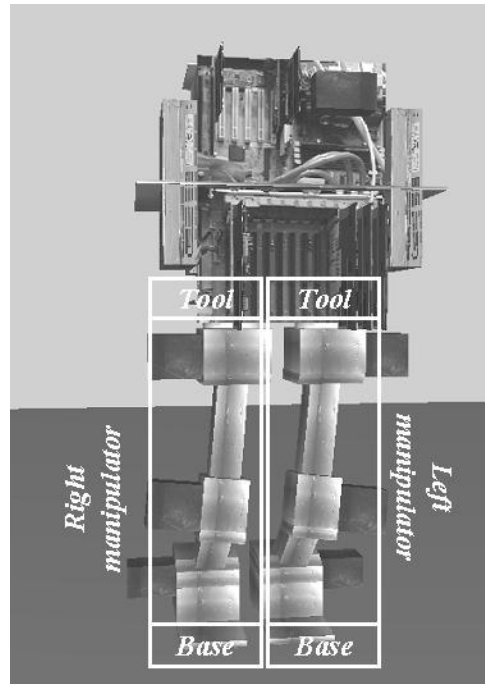


Figure 5.14. The robot in the double support phase can be regarded as a trunk manipulated by two six-DOF manipulators based on the ground.

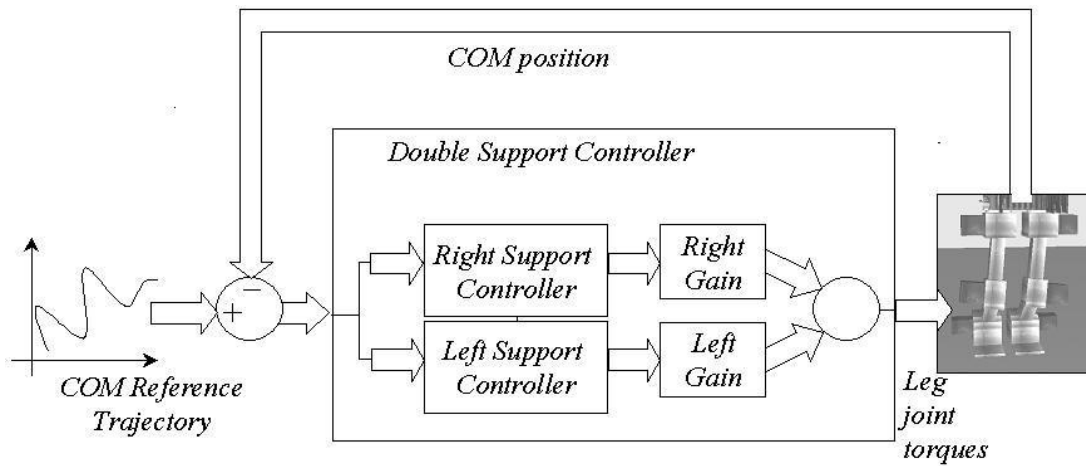


Figure 5.15. The double support phase controller structure.

The robot in swing phases can be seen as a ground based manipulator controlling the CoM position and trunk orientation and a second manipulator based at the hip controlling the swing foot position and orientation, as shown in Fig. 5.16. The right support (Fig. 5.17) and left swing (Fig. 5.18) controllers are activated simultaneously. The single support controller applies the position control scheme described above for the double support phase (without using the scaling factors). The swing leg controller is a stiffness controller for the foot position and orientation. For soft landing purposes, a Cartesian stiffness matrix with low stiffness against in orientation errors and position errors in the z-direction is employed. The horizontal directions are penalized with higher stiffness coefficients. These choices enable crisp landing positions with minimal impact disturbance.

As shown in figures 5.19 and 5.20 the controllers in the left support and right swing phase are identical to the controllers in the right support and left swing phase.

Chapter 7 presents simulation results with the references and controller structures outlined in this chapter.

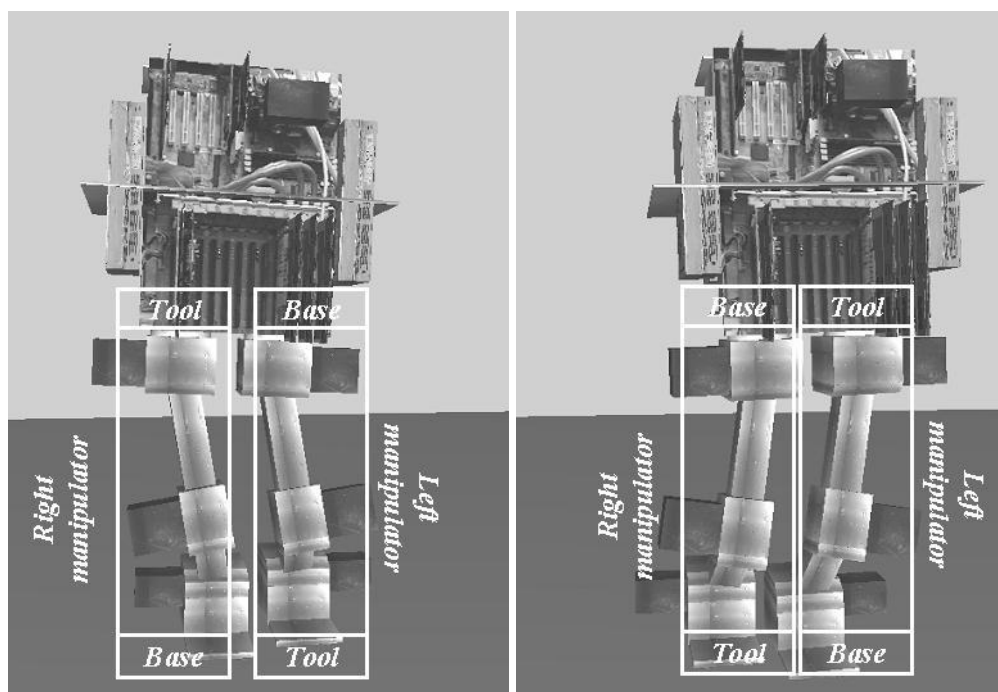


Figure 5.16. The robot in swing phases can be seen as a ground based manipulator and a second manipulator based at the hip.

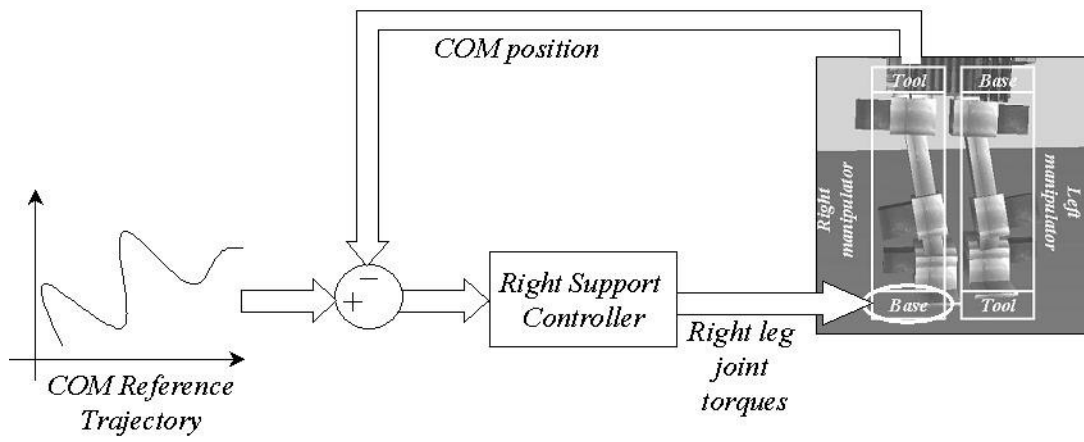


Figure 5.17. The single support controller for the right foot.

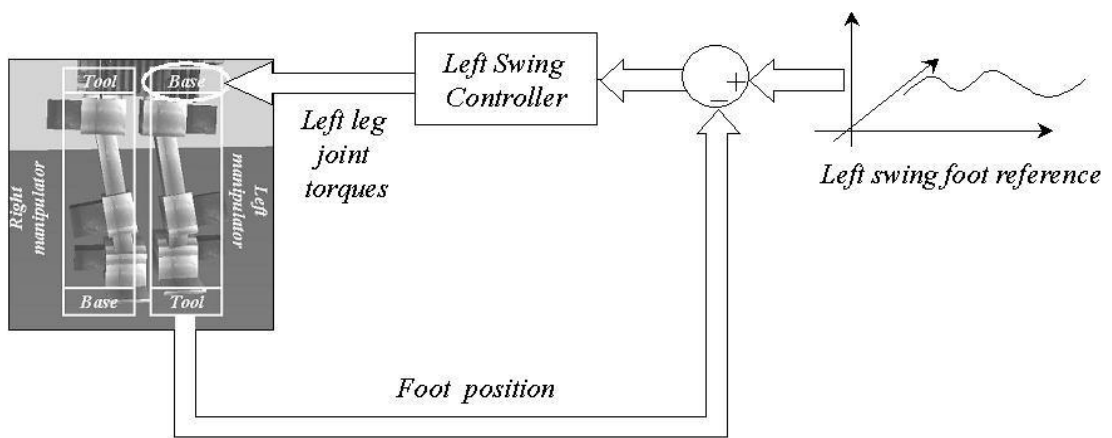


Figure 5.18. The swing controller for the left foot.

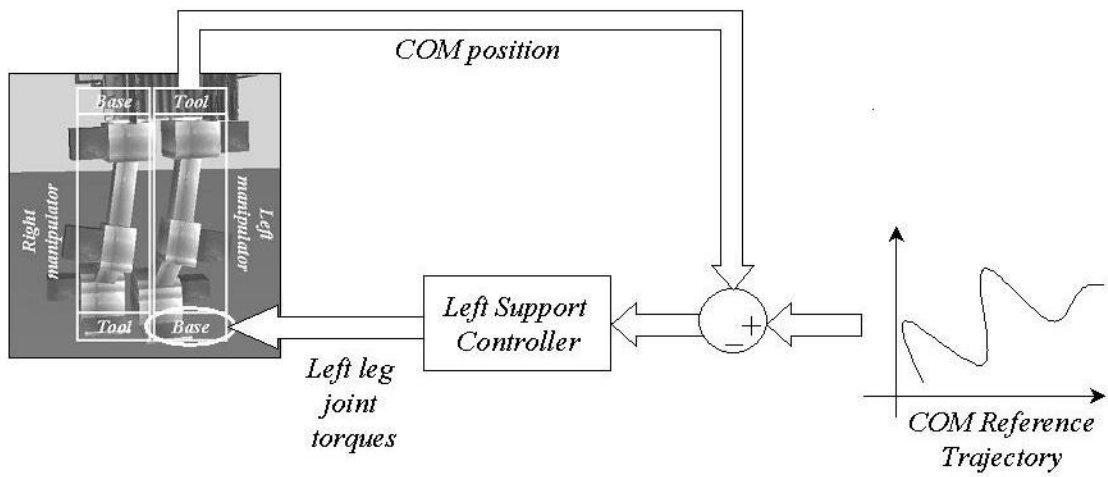


Figure 5.19. The single support controller for the left foot.

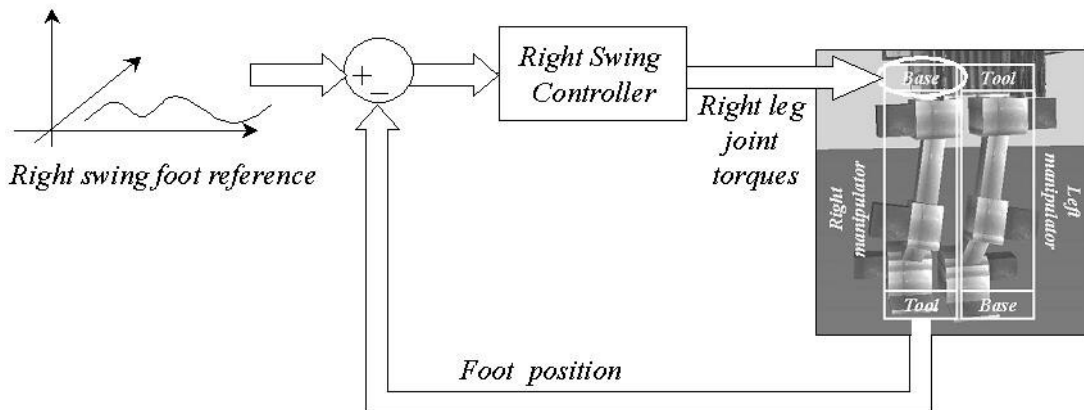


Figure 5.20. The swing controller for the right foot.

Chapter 6

6. THE BIPED MODEL and SIMULATION RESULTS

6.1 The Biped Model as the Simulation Test Bed

The biped model used in this work as a simulation test bed is called “Mari-2”, one of the biped robots of Yokohama National University, Japan [11] (Fig. 6.1).

This model is selected since it is an experimentally tested model and suitable for our simulations. The test bed consists of two 6-DOF legs and a trunk connecting them. Three joint axes are positioned at the hip. Two joints are in the ankle and one at the knee. Approximate link sizes and the masses of the biped are given in Table 6.1.

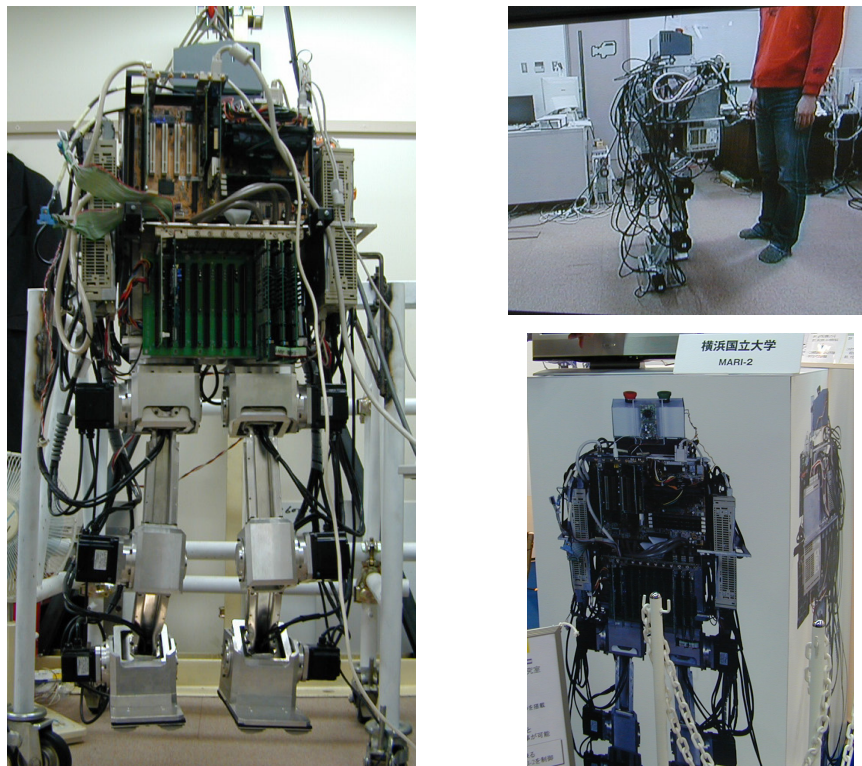


Figure 6.1. Some pictures of the used test bed robot, Mari-2.

Table 6.1. Masses and dimensions of the biped robot links.

Link	Dimensions (LxWxH) [m]				Mass [kg]	
Trunk	0.2	x	0.4	x	0.5	50
Thigh	0.1	x	0.1	x	0.1	12
Calf	0.22	x	0.05	x	0.1	0.5
Foot	0.1	x	0.12	x	0.25	5.5

The joint axis assignment with the Denavit-Hartenberg convention in [14] is shown in Chapter 2, Fig. 2.8, and the Denavit-Hartenberg parameters of the legs are listed at Table 6.2.

Table 6.2. D-H Parameters of the biped leg.

Link	a_i	α_i	d_i	θ_i
1	0	$\frac{\pi}{2}$	0	θ_1^*
2	0	$-\frac{\pi}{2}$	0	θ_2^*
3	L_3	$\frac{\pi}{2}$	0	θ_3^*
4	L_4	0	0	θ_4^*
5	0	$-\frac{\pi}{2}$	0	θ_5^*
6	L_6	0	0	θ_6^*

The general form of the dynamic model used for the bipedal robot is as shown in (2.4). The simulation scheme is similar to the one in [31,32], which generalize the recursive Newton-Euler dynamic modeling method in [33,34] to the tree structure. The details of the simulation algorithm and contact modeling can be found in [35].

The simulations are implemented in Simulink with sampling time of 0.5 milliseconds with Euler integration. In order to visualize the walking, simulation results are animated using an OpenGL based animation environment. A snapshot of the animation is shown in Fig. 6.2.

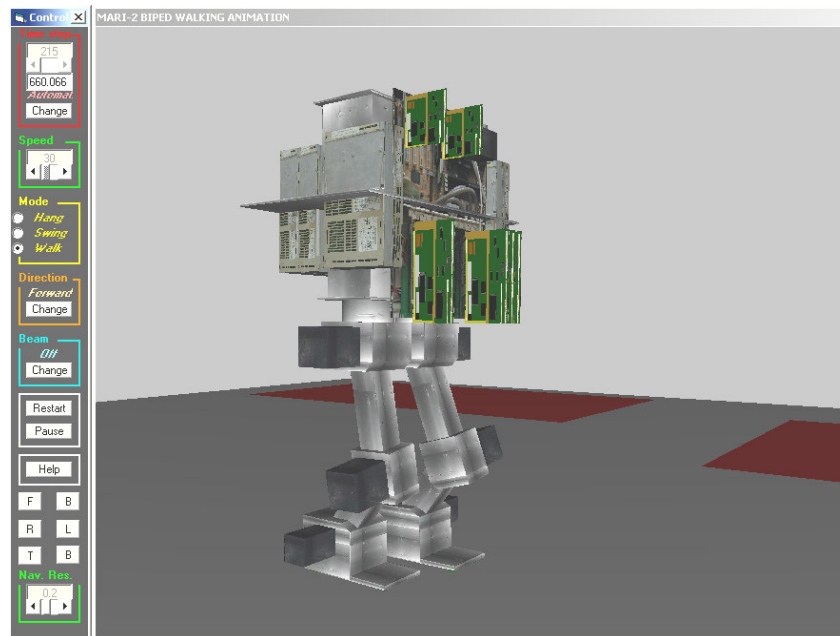


Figure 6.2. A screen shot from the Biped Animation.

6.2 The Simulation Results

Simulations studies are carried out with the robot model described in Chapter 2, references generated in Chapter 4 and the coordination and control mechanism discussed in Chapter 5. Various parameters used for reference generation and control are presented in tables 6.3-6.5.

Table 6.3. Some of the important simulation parameters.

<i>Parameter</i>	<i>Value</i>
<i>x</i> -reference foot-CoM offset	-0.06 m
Step height	0.02 m
Step period	3 s
Step size	0.2 m
Foot to foot <i>y</i> -direction distance	0.08 m
Foot to foot <i>y</i> -direction ZMP reference distance	0.1 m
Ground interaction threshold force	100 N

Table 6.4. PID controller gains for support leg joints.

<i>Joint Number</i>	K_p	K_d	K_i
1 (Hip)	6000	1	40
2	20000	1	40
3	20000	1	40
4	30000	1	40
5	30000	1	40
6 (Ankle)	6000	1	40

Table 6.5. Stiffness Control Gains for Swing Leg Controllers.

<i>Cartesian Error Direction</i>	<i>Cartesian Stiffness Gain</i>	<i>Cartesian Damping Gain</i>
x	5000	5
y	5000	5
z	20000	20
Roll	100	1
Pitch	100	1
Yaw	100	1

Fig. 6.3 shows the y-direction CoM and CoM reference for a 8 seconds walk. It can be observed that the CoM reference in this direction is closely tracked except in the single support phases. The y-direction ZMP and ZMP reference curves displayed in Fig. 6.4 also a deviation from the reference curve in the swing phases. This suggests that the simple LIMP model, concentrating on the robot trunk, and ignoring the effects of the swing foot on the CoM of the whole robot, may encounter problems when the leg weight is not very low. The MARI-2 legs weigh 15 kg. Although much less than the 50 kg trunk weight, this weight affects the y-direction CoM and ZMP curves significantly. Apart from the swing phases, the tracking performance is quite acceptable.

The x-direction CoM and ZMP curves together with their references are presented in figures 6.5 and 6.6, respectively. These curves, too, display oscillations and deviations from reference curves mainly due to the trunk dominated LIMP model. Still, in the average, the reference curves are tracked.

Figures 6.7 and 6.8 show the x-y-plane trajectories of the CoM and ZMP, respectively. The reference curves are displayed in these figures too. The tracking behavior seen in Fig. 6.7 is an acceptable one, whereas the ZMP curve in Fig 6.8 shows high amplitude oscillations in both directions. The more oscillatory behavior of the ZMP can be due to the ground force modeling which is based on an adaptive spring penalty approach [35]. Again, the worsening effect of the swing foot dynamics not modeled in the reference generation algorithm can be observed in Fig. 6.8. It can also be seen that the actual ZMP is frequently concentrated at the foot edges. This is an expected result for support legs under position control. They are controlled as they are bolted down to the ground. However actually they are free to move and the incline to some extent, pushing the ZMP to the foot edges.

In the average, the ZMP curve moves forward even in the single support phases. However, the transient behavior does not indicate that the naturalness of the human walk is achieved completely.

Although there are some tracking problems as discussed above, the reference generation and control algorithms are generally successful, keeping the ZMP in the support polygon and enabling the robot move forward with an almost constant speed of 7 cm per second. This is achieved without the need for the elaborate trial and error steps common to many other reference generation approaches.

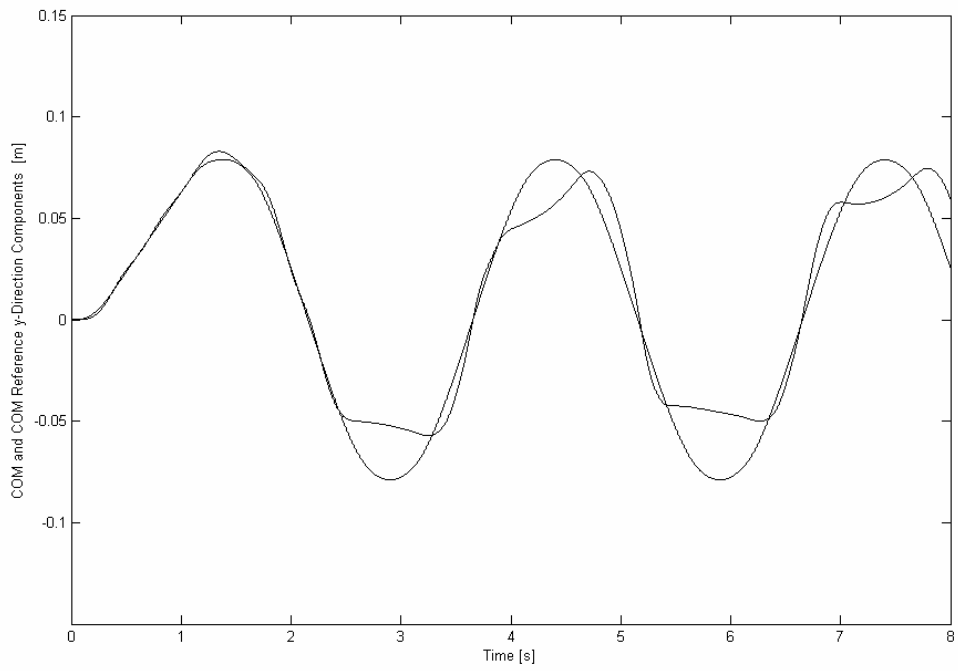


Figure 6.3. CoM and CoM reference y-direction components.

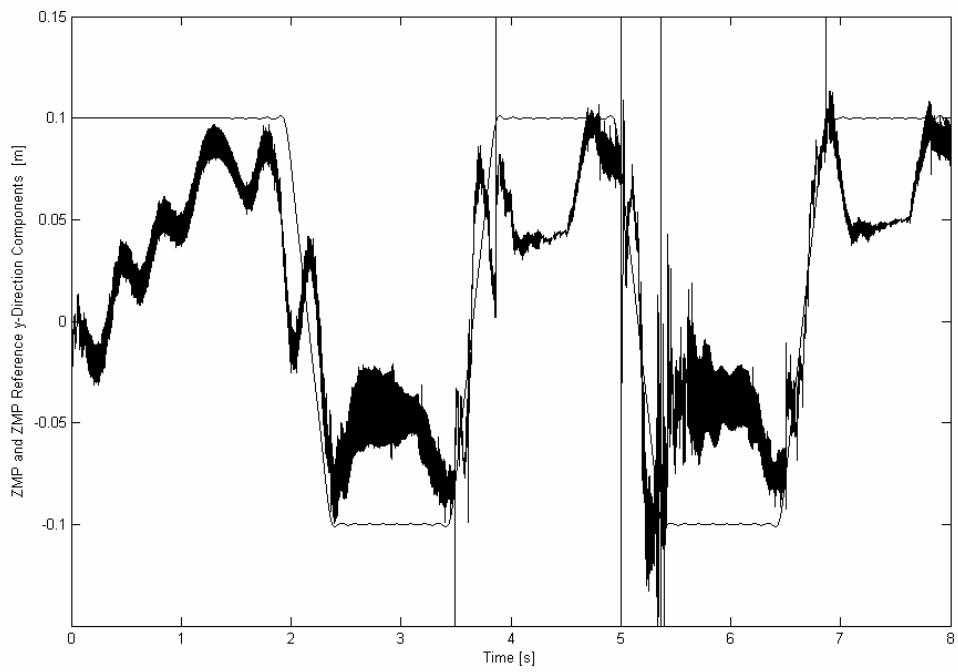


Figure 6.4. ZMP and ZMP reference y-direction components.

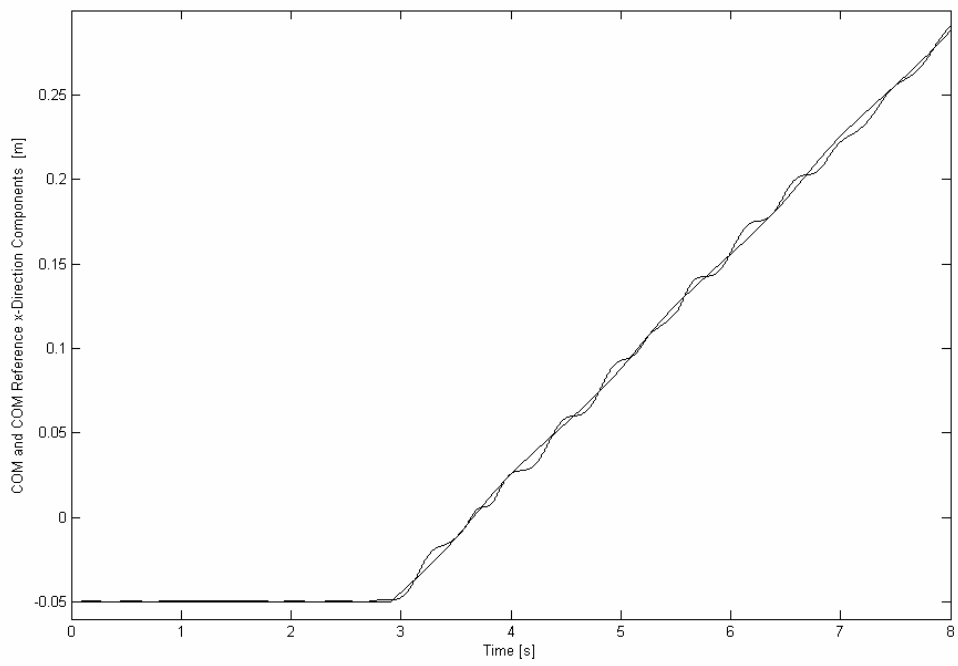


Figure 6.5. CoM and CoM reference x -direction components.

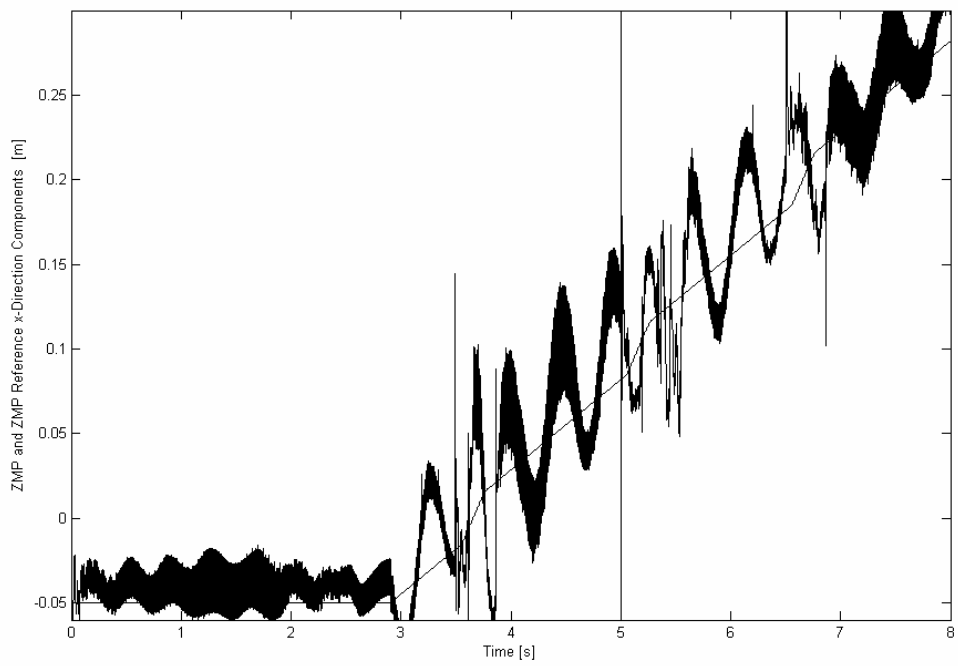


Figure 6.6. ZMP and ZMP reference x -direction components.

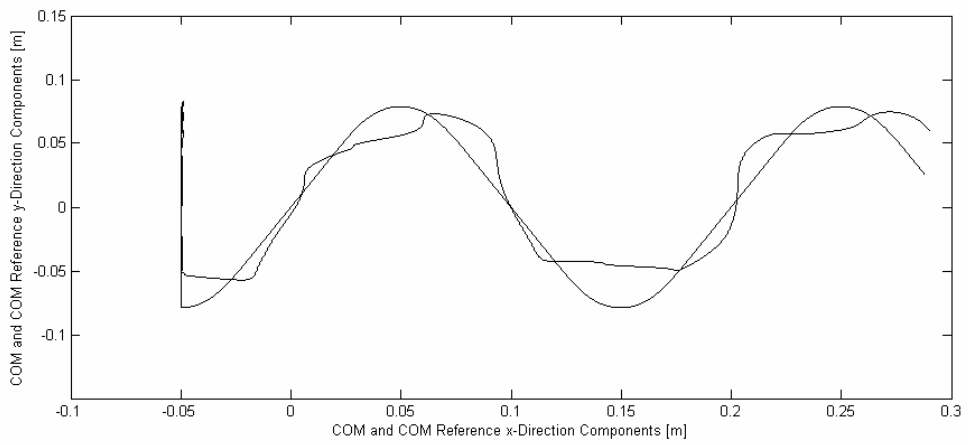


Figure 6.7. CoM and CoM reference on the x - y -plane.

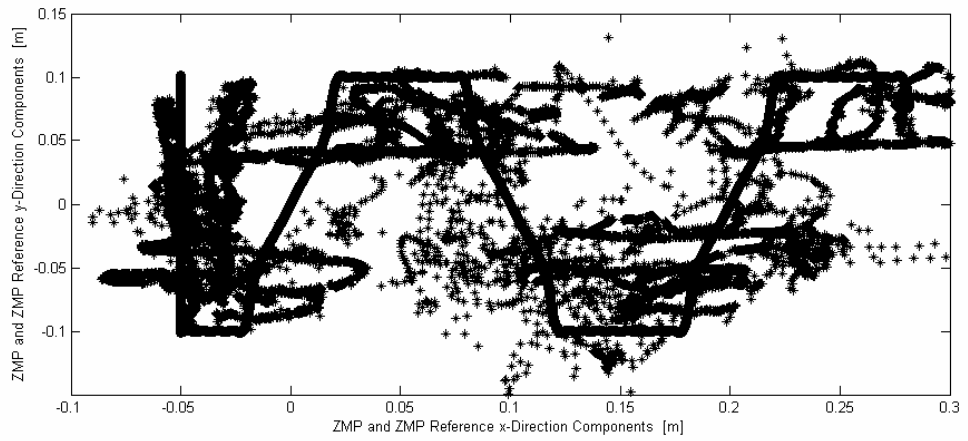


Figure 6.8. ZMP and ZMP reference on the x - y -plane.

7. CONCLUSION and FUTURE WORK

A trajectory generation, coordination and control approach for biped walking robots is presented in this thesis. The reference generation part is based on the Linear Inverted Pendulum Model. As a novel approach, human-like ZMP reference trajectories with double support phases are used with existing Fourier series approximation techniques for the solution of Linear Inverted Pendulum Model. The approximated solution to LIPM dynamics equations are employed in order to achieve naturalness in the walk. A control structure consisting of different modes and position and force control techniques is developed too.

Simulation and animation studies have shown that the reference generation without considering the effects of the swing foot on robot ZMP can lead to significant deviations from reference trajectories. ZMP trajectories concentrating at the inside edges of the swing feet suggest that there is room for improvement at the controller side too.

The next step would be to develop online indirect ZMP controller algorithms to modify the dynamics of the robot to compensate for the disturbance of each swinging leg and preserve a dynamically stable walk. Such an algorithm should force the measured ZMP to follow the reference natural ZMP by doing several modifications in the motion of, say CoM, the walking robot. These modifications can also regard changes in the parameters of the walking algorithm such as changing the stride distance or foot-to-foot distance. Furthermore, the robustness of the contact modeling can be considered and revisions can be made to get better results. Experiments show that small impacts that occur at each stepping movement effects the quality of the walking algorithm since the force at each foot is a parameter for the walking algorithm. Yet the walk, however, is stable and this is a very promising result making the whole algorithm a candidate for implementation.

8. APPENDIX

The following Matlab code is the reference generation algorithm that is used for CoM.

```
% naturalCoMtrajectory.m
%-----
close all
clear all
A=.2;           %Stride Length
B=.8;           %Foot-to-Foot Distance
wn=sqrt(10);
T0=1;           %Stepping Period
b=.14;          %Foot Sole length
t=0:0.001:10;
DSparam=20 % DSparam is the double support phase parameter that
           % defines the double support time

% % NATURAL CX calculation

c1=0;
for n=1:24
    c1 = c1 + [[(B-2*b)*sinc(n*pi/DSparam)*T0^2*wn^2*(1+
cos(n*pi))]] / [n*pi*(T0^2*wn^2 + n^2*pi^2)]*sin(n*pi*t/T0);
end

cx_new= (B/T0)*(t-T0/2) + c1;

hold on
plot(t,cx_new,'r')

%-----
% NATURAL PX calculation

p11=0;
p12=0;

for n=1:24
```

```

        p11 = p11 + [[[B2*b)*sinc(n*pi/DSparam)*T0^2*wn^2*(1+cos(n*pi))]]
/ [n*pi*(T0^2*wn^2 + n^2*pi^2)]]*sin(n*pi*t/T0)*(1+n^2*pi^2/
(T0^2*wn^2));
    end
    f=p11 ;
    px_new = f - B*(1/2 - t/T0);

    plot(t,px_new,'b')
    %-----
    % Line wise ZMP reference
    c = (B-2*b)*floor(t/T0).*st(t-T0)/T0;
    y = 2*b*(t)/T0 + c -b;%Linewise ZMP(without double support phase)

    hold on
    plot (t,y,'k')

    %-----
    %      OLD CX      calculation
    cx_old=0;

    for n=1:24
        cx_old = cx_old + [[[B*T0^2*wn^2*(1+ cos(n*pi))]] /
[n*pi*(T0^2*wn^2 + n^2*pi^2)]]*sin(n*pi*t/T0);
    end

    cx_old= (B/T0)*(t-T0/2)+ cx_old;
    hold on
    plot(t,cx_old,'b')
    %-----
    %      OLD CY      calculation

    cy_old=0;

    for n=1:24
        cy_old = cy_old + [[[2*A*T0^2*wn^2*(1- cos(n*pi))]] /
[n*pi*(T0^2*wn^2 + n^2*pi^2)]]*sin(n*pi*t/T0);
    end
    hold on
    plot(t,cy_old,'b')

```

```

%-----
%      NATURAL PY calculation

p2=0;

for n=1:24
    p2 = p2 + [[2*A*sinc(n*pi/Dsparam)*T0^2*wn^2*(1-cos(n*pi))] /
[n*pi*(T0^2*wn^2 + n^2*pi^2)]]*sin(n*pi*t/T0)*(1+n^2*pi^2/(T0^2*wn^2));
end

py_new=p2;

hold on
plot(t,py_new,'r')

%      NATURAL CY calculation

cy_new=0;

for n=1:24

    cy_new = cy_new + [[2*A*sinc(n*pi/Dsparam)*T0^2*wn^2*(1-
cos(n*pi))] / [n*pi*(T0^2*wn^2 + n^2*pi^2)]]*sin(n*pi*t/T0);
end

hold on

plot(t,cy_new,'r')

```

REFERENCES

- [1] Jerry, P., Gill, P. “ Intuitive Control of a Planar Bipedal Walking Robot”, *IEEE Proceedings of the IEEE International Conference on Robotics & Automation, Leuven Belgium*, May 1998.
- [2] Franc, P., Grizzle, J.W., Abba, G. “ Stable Walking of a 7-DOF Biped Robot”, *IEEE Transactions on Robotics and Automation*, vol.19, No.4, pp.653-668, August 2003.
- [3] Sakagami, Y., Watanabe, R., Aoyama, C., Shinichi, M., Higaki, N., Fujimura, K., “The intelligent ASIMO: System overview and integration”, *Proceedings of the IEEE International Conference on Intelligent Robots and Systems*, Lausanne, Switzerland, October 2002
- [4] Endo, G., Nakanishi, J., Morimoto, J., and Cheng, G., “ Experimental Studies of a Neural Oscillator for Biped Locomotion with QRIO”, *Proceedings of the IEEE International Conference on Robotics and Automation*, pp.596-602, Barcelona, Spain, April 2005
- [5] Sawada, T., Takagi, T. and Fujita, M., “Behavior Selection and Motion Modulation in Emotionally Grounded Architecture for QRIO SDR-4X II”, *Proceedings of the IEEE International Conference on Intelligent Robots and Systems*, vol.3, pp. 2514-2519, Sendai, Japan, October 2004.
- [6] Lohmeier, S., Löffler, K., Gienger, M., Ulbrich, H., Pfeiffer, F., “Computer System and Control of Biped “Johnnie””, *Proceedings of the IEEE International Conference on Robotics and Automation*, vol.4, pp.4222-4227, New Orleans, LA, April 2004.
- [7] Kaneko, K., Kanehiro, F., Kajita, S., Yokoyama, K., Akachi, K., Kawasaki, T., Ota, S., Isozumi, T., “Design of Prototype Humanoid Robotics Platform for HRP”, *IEEE International Conference on Intelligent Robots and Systems*, pp.2431-2436, vol.3, October 2002.
- [8] Kajita, S., Kanehiro, K., Kaneko, K., Fujiwara, K., Yokoi, K., Hirukawa, H.,” A Real Time Pattern Generator for Bipedal Walking” *Proceedings of the IEEE*

- International Conference on Robotics and Automation, vol.1, pp.31-37, May 2002.*
- [9] Vukobratovic, M., Borovac, B., Surla, D. and Stokic, *Biped Locomotion: Dynamics, Stability and Application*. Springer-Verlag, 1990.
- [10] Dasgupta, A., Nakamura, Y. “Making Feasible Walking Motion of Humanoid Robots from Human Motion Capture Data” *Proceedings of the IEEE International Conference on Robotics and Automation*, Detroit, Michigan, May 1999.
- [11] Erbatur, K., A. Okazaki, K. Obiwa, T. Takahashi and A. Kawamura, “A Study on the Zero Moment Point Measurement for Biped Walking Robots”, *Proc. 7th International Workshop on Advanced Motion Control, pp. 431-436, Maribor, Slovenia, 2002*
- [12] Whittle, M.W., “Gait Analysis: an introduction” , Butterworth-Heinemann 2001
- [13] Winter, D.A., “The biomechanics and motor control of human gait: normal, elderly and pathological”, Waterloo Biomechanics 1991.
- [14] Spong, M., M. Vidyasagar, ”Robot Dynamics and Control”, John Wiley and Sons, 1989.
- [15] www.humanoid.waseda.ac.jp/booklet/kato02.html
- [16] www.inl.gov/adaptiverobotics/humanoidrobotics/leggedlocomotion.shtml
- [17] www.technet.pnl.gov/dme/robotics/manny.stm
- [18] Marc Raibert, *Legged Robots that Balance*, MIT Press, Cambridge, MA, 1986.
- [19] Huang, Q., Kajita, S., Koyachi, N., Kaneko, K., Yokoi, K., Arai, H., Komoriya, K., Tanie, K., “A High Stability, Smooth Walking Pattern for a Biped Robot”, *Proceedings of IEEE International Conference on Robotics and Automation, pp: 65-71 vol.1, Detroit, Michigan, May 1999*
- [20] Nishiwaki, K., Nagasaka, K., Inaba, M., Inoue, H., “Generation of Reactive Stepping Motion for a Humanoid by Dynamically Stable Mixture of Pre-designed Motions” *SMC’99 Proceedings of the Conference on Systems, Man and Cybernetics, pp: 902-907 vol.6, Oct. 1999.*
- [21] Yamaguchi, J., Soga, E., Inoue, S., Takanishi, A., “Development of a Bipedal Humanoid Robot – Control Method of Whole Body Cooperative Dynamic Biped Walking-“ *Proceedings of IEEE International Conference on Robotics and Automation, pp: 368-374 vol.1, Detroit, Michigan, May 1999.*

- [22] Kajita, S., Tani, K. “Study of Dynamic Biped Locomotion on Rugged Terrain – Theory and Basic Experiment–“ *ICAR, Fifth International Conference on Advanced Robotics*, pp: 741-746, vol.1, June 1991.
- [23] Sano, A., Furusho, J., “Realization of Natural Dynamic Walking Using the Angular Momentum Information” *IEEE International Conference on Robotics & Automation*, pp: 1476 – 1481, vol.3, May 1990.
- [24] Park, H.J., Kim, D.K., “Biped Robot Walking Using Gravity Compensated Linear Inverted Pendulum Mode and Computed Torque Control” *Proceedings of IEEE International Conference on Robotics and Automation*, pp: 3528 - 3533, vol.4, May 1998.
- [25] Kajita, S., Matsumoto, O., Saigo, M., “Real time 3D Walking Pattern Generation for a Biped Robot With Telescopic Legs” *Proceedings of IEEE International Conference on Robotics and Automation*, pp: 2299 - 2306, vol.3, 2001.
- [26] Sugihara, T., Nakamura, Y., Inoue, H., “Real-time Humanoid Motion Generation Through ZMP Manipulation based on Inverted Pendulum Control”, *Proceedings of IEEE International Conference on Robotics and Automation*, pp: 1404 - 1409, vol.2, Washington DC, May 2002.
- [27] Kajita, S., Kahehiro, F., Kaneko, K., Fujiwara, K., Harada, K., Yokoi, K., Hirukawa, H., “ Biped Walking Pattern Generation using Preview Control of the Zero-Moment-Point”, *Proceedings of IEEE International Conference on Robotics and Automation*, pp: 1620 - 1626, vol.2, Taipei, Taiwan, September 2003.
- [28] Okumura, Y., Tawara, T., Endo, K., Furuta, T., Shimizu, M., “Real-time ZMP Compensation for Biped Walking Robot using Adaptive Inertia Force Control”, *Proceedings of IEEE International Conference on Intelligent Robots and Systems*, pp: 335 – 339, vol.1, Las Vegas, Nevada, Oct 2003.
- [29] Choi, Y., You, B.J., Oh, S.R., “On the Stability of Indirect ZMP Controller for Biped Robot Systems”, *Proceedings of International Conferenc on Intelligent Robots and Systems*, pp: 1966 - 1971, vol.2, Sendal, Japan, June 2004.
- [30] Zhu, C., Tomizawa, Y., Luo, X., Kawamura, A. “Biped Walking with Variable ZMP, Frictional Constraint, and Inverted Pendulum Model”, *IEEE International Conference on Robotics and Biomimetics*, pp: 425 – 430, Shenyang, China Aug 2004.

- [31] Fujimoto, Y, "Study on Biped Walking Robot with Environmental Force Interaction", *Doctoral Thesis submitted to Division of Electrical and Computer Engineering, Graduate School of Engineering, Yokohama National University*, March 1998.
- [32] Fujimoto, Y., A. Kawamura, "Simulation of an Autonomous Biped Walking Robot Including Environmental Force Interaction", *IEEE Robotics and Automation Magazine*, pp. 33-42, June 1998.
- [33] R. Featherstone, *Robot Dynamics Algorithms*. Kluwer Academic Publishers, 2003.
- [34] Luh, J.Y.S., M. W. Walker and R.P.C. Paul, "On-line Computational Scheme for Mechanical Manipulators," *Jour. Dyn. Syst. Meas. Cont.*, Vol. 102, pp. 69, June 1980.
- [35] Erbatur, K. and A. Kawamura, "A New Penalty Based Contact Modeling and Dynamics Simulation Method as Applied to Biped Walking Robots," *Proc. 2003 FIRA World Congress*, October 1-3, 2003 Vienna, Austria